

AD-A126 838

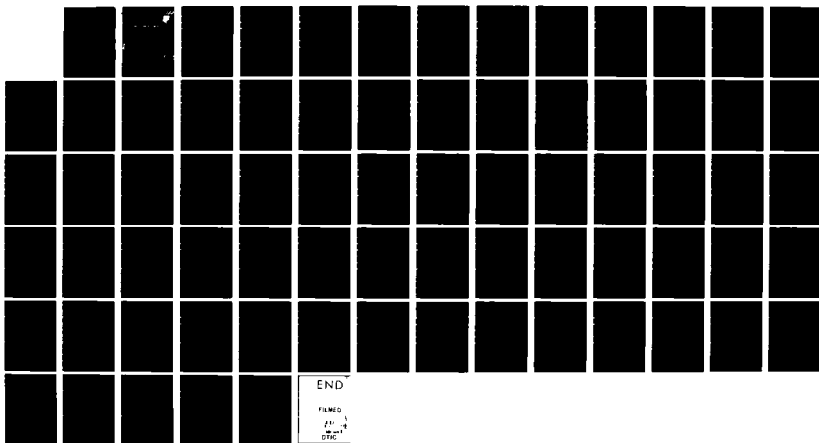
ANGLE OF ARRIVAL ESTIMATION(U) OHIO STATE UNIV COLUMBUS  
ELECTROSCIENCE LAB B V ANDERSSON DEC 82 ESL-711679-4  
RADC-TR-82-258 F38682-79-C-8868

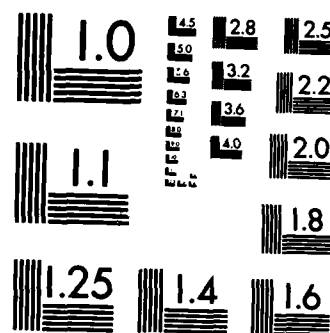
1/1

UNCLASSIFIED

F/G 17/2

NL





MICROCOPY RESOLUTION TEST CHART  
NATIONAL BUREAU OF STANDARDS-1963-A

ADA 126038

**RADC-TR-82-250**  
**Interim Report**  
**December 1982**



## **ANGLE OF ARRIVAL ESTIMATION**

**The Ohio State University**

**Bengt V. Andersson**

**APPROVED FOR PUBLIC RELEASE; DISTRIBUTION UNLIMITED**

DTIC FILE COPY

**DTIC**  
**ELECTE**  
**S** MAR 24 1983

**D**

**ROME AIR DEVELOPMENT CENTER**  
**Air Force Systems Command**  
**Griffiss Air Force Base, NY 13441**

83 03 24 021

83 03 24 001

This report has been reviewed by the RADC Public Affairs Office (PA) and is releasable to the National Technical Information Service (NTIS). At NTIS it will be releasable to the general public, including foreign nations.


RADC-TR-82-250 has been reviewed and is approved for publication.

APPROVED:



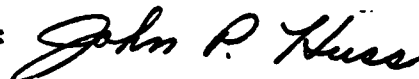
STUART H. TALBOT  
Project Engineer

APPROVED:



BRUNO BEEK  
Technical Director  
Communications Division

FOR THE COMMANDER:



JOHN P. HUSS  
Acting Chief, Plans Office

If your address has changed or if you wish to be removed from the RADC mailing list, or if the addressee is no longer employed by your organization, please notify RADC (DCCR) Griffiss AFB NY 13441. This will assist us in maintaining a current mailing list.

Do not return copies of this report unless contractual obligations or notices on a specific document requires that it be returned.

UNCLASSIFIED

SECURITY CLASSIFICATION OF THIS PAGE (When Data Entered)

REPORT DOCUMENTATION PAGE		READ INSTRUCTIONS BEFORE COMPLETING FORM
1. REPORT NUMBER RADC-TR-82-250	2. GOVT ACCESSION NO. AD-4126	3. RECIPIENT'S CATALOG NUMBER 038
4. TITLE (and Subtitle)  ANGLE OF ARRIVAL ESTIMATION		5. TYPE OF REPORT & PERIOD COVERED Interim Report Apr 80 - Apr 81
		6. PERFORMING ORG. REPORT NUMBER ESL 711679-4
7. AUTHOR(s)  Bengt V. Andersson		8. CONTRACT OR GRANT NUMBER(s)  F30602-79-C-0068
9. PERFORMING ORGANIZATION NAME AND ADDRESS The Ohio State Univ. Electrosience Laboratory Department of Electrical Engineering Columbus OH 43212		10. PROGRAM ELEMENT, PROJECT, TASK AREA & WORK UNIT NUMBERS 62702F 45196308
11. CONTROLLING OFFICE NAME AND ADDRESS  Rome Air Development Center (DCCR) Griffiss AFB NY 13441		12. REPORT DATE December 1982
		13. NUMBER OF PAGES 48
14. MONITORING AGENCY NAME & ADDRESS (if different from Controlling Office)  Same		15. SECURITY CLASS. (of this Report)  UNCLASSIFIED
		15a. DECLASSIFICATION/DOWNGRADING SCHEDULE N/A
16. DISTRIBUTION STATEMENT (of this Report)  Approved for public release; distribution unlimited.		
17. DISTRIBUTION STATEMENT (of the abstract entered in Block 20, if different from Report)  Same		
18. SUPPLEMENTARY NOTES  RADC Project Engineer: Stuart H. Talbot (DCCR)		
19. KEY WORDS (Continue on reverse side if necessary and identify by block number)  Angle of Estimation                      TDMA SATCOM System Monopulse System                      Maximum Likelihood Theory Adaptive Array Covariance Matrix		
20. ABSTRACT (Continue on reverse side if necessary and identify by block number)  The objective of this study was to develop methods of determining the angle of arrival of uplink signals in a Time Division Multiple Access (TDMA) Satellite Communications System that employs high gain, switchable downlink spotbeams. Two approaches are examined and data resulting from theoretical calculations and computer simulations are presented from comparison. Both approaches are based upon maximum likelihood estimation and incorporate adaptive array processing in suppressing undesired signals.		

DD FORM 1 JAN 73 1473 EDITION OF 1 NOV 65 IS OBSOLETE

UNCLASSIFIED

SECURITY CLASSIFICATION OF THIS PAGE (When Data Entered)

UNCLASSIFIED

SECURITY CLASSIFICATION OF THIS PAGE(When Data Entered)

The results show that either approach can accurately determine the angle of arrival of a desired signal in the presence of much higher powered undesired signals.

In future TDMA SATCOM Systems, the angle of arrival data could be provided to expanded on-board processors to steer the switchable, downlink spotbeams.

Accession For	
NTIS GRA&I	<input checked="checked" type="checkbox"/>
DTIC TAB	<input type="checkbox"/>
Unannounced	<input type="checkbox"/>
Justification	
By	
Distribution/	
Availability Codes	
Dist	Avail and/or Special
F	



UNCLASSIFIED

SECURITY CLASSIFICATION OF THIS PAGE(When Data Entered)

## TABLE OF CONTENTS

	Page
LIST OF FIGURES	v
1. INTRODUCTION	1
2. MAXIMUM LIKELIHOOD ESTIMATES OF THE AoA	3
2.1 The Likelihood Function for a Linear Array of Isotropic Elements	5
2.2 The Monoestimator	9
2.3 The Q-Estimator	11
3. SYSTEM ASPECTS AND SIMULATION	16
3.1 The Simulation Model	16
a) Generation of the antenna element signals	16
b) Generation of the covariance matrix	18
c) Angle of Arrival Estimation	19
3.2 System Aspects	19
3.3 Assumptions in the Simulation	21
4. SIMULATED RESULTS AND DISCUSSION	22
4.1 Known Covariance Matrix	23
a) AoA Estimation in the Absence of all Jammers	23
b) AoA Estimation in the Presence of One Jammer	26
c) AoA Estimation in the Presence of Two Jammers	43

	Page
4.2 Estimated Covariance Matrix	48
a) AoA Estimation in the Absence of All Jammers	49
b) AoA Estimation in the Presence of One Jammer	49
c) AoA Estimation in the Presence of Two Jammers	54
5. SUMMARY AND CONCLUSIONS	61
REFERENCES	63



## LIST OF FIGURES

Figure		Page
1.	Estimated AoA as a function of the assumed AoA for the monoestimator.	24
2.	Q-function versus $(\theta - \theta_s)$ .	25
3.	Estimated AoA using a 5 element array, spaced $2.5\lambda$ apart as a function of the angular distance between one jammer at $\theta_j$ and the desired signal at $\theta_s = 0^\circ$ .	27
4.	Estimated AoA using a 10 element array spaced $1.25\lambda$ apart as a function of the angular distance between one jammer at $\theta_j$ and the desired signal at $\theta_s = 0^\circ$ .	29
5.	Estimated AoA using a 5 element array as a function of the angular distance between one jammer at $\theta_j$ and the desired signal at $\theta_s = 0^\circ$ .	30
6.	Estimated AoA using a 5 element array as a function of the angular distance between one jammer at $\theta_j$ and the desired signal at $\theta_s = 0^\circ$ .	31
7.	Plots of Q-function, averaged over 10 samples, for different scenarios.	33
8.	Estimated AoA using a 5 element array as a function of the angular distance between one jammer at $\theta_j$ and the desired signal at $\theta_s = 0^\circ$ .	34

Figure		Page
9.	Sum and difference patterns for a 5 element array with inter-element spacing $2.5\lambda$ .	35
10.	Sum and difference patterns for a 5 element array with inter-element spacing $2.5\lambda$ .	36
11.	Sum and difference patterns for a 5 element array with inter-element spacing $2.5\lambda$ .	37
12.	Sum and difference patterns for a 5 element array with inter-element spacing $2.5\lambda$ .	38
13.	Sum and difference patterns for a 5 element array with inter-element spacing $2.5\lambda$ .	39
14.	Sum and difference patterns for a 5 element array with inter-element spacing $2.5\lambda$ .	40
15.	Sum and difference patterns for a 5 element array with inter-element spacing $2.5\lambda$ .	41
16.	Estimated AoA in the presence of two jammers using a 5 element array as a function of second jammer direction.	44
17.	Plots of the Q-function averaged over 10 samples and estimated AoA for different scenarios.	45
18.	Plots of the Q-function averaged over 10 samples.	46
19.	Plots of the Q-function averaged over 10 samples, and estimated AoA for different scenarios.	47
20.	Estimated AoA as a function of the assumed AoA for the monoestimator.	50

Figure		Page
21.	Q-function versus $\theta$ for 5 element array.	51
22.	$Q_1$ -function versus $\theta$ for 5 element array.	52
23.	Q-function versus $\theta$ for 5 element array in the presence of one jammer.	53
24.	Q-function versus $\theta$ for 5 element array in the presence of one jammer.	55
25.	Q-function versus $\theta$ for 5 element array in the presence of one jammer.	56
26.	Q-function versus $\theta$ for 5 element array in the presence of two jammers.	57
27.	Q-function versus $\theta$ for 5 element array in the presence of two jammers.	59
28.	Q-function versus $\theta$ for 5 element array in the presence of two jammers.	60

## 1. INTRODUCTION

The objective of this study has been to develop an angle of arrival estimation technique that would perform reliably in the presence of high powered jammers which are stronger by up to several orders of magnitude than the desired signal whose angle is to be estimated. The angle estimate is aimed at a demand assignment TDMA SATCOM system employing high gain switchable downlink beams. A high accuracy angle estimate would permit the establishment of a reliable communication link whose quality would greatly exceed that of a system employing an earth coverage beam.

Various approaches have been used to accomplish angle of arrival (AoA) estimation, the best known is the monopulse system. The monopulse system provides a good AoA estimate as long as the noise is limited to receiver noise or uniformly distributed background noise. The presence of strong directional interfering signals (jammers) would drastically degrade the estimation, however, and the monopulse system would no longer be useful.

Adaptive arrays are ideally suited for the suppression of jammers and the maximization of signal to interference plus noise ratios. It would thus appear to be very advantageous if an angle of arrival estimation system would incorporate an adaptive array in its processor. Indeed, Davis, et. al., [1] extended the theory of adaptive array to the angle estimation problem. Based on the maximum likelihood theory of angle estimation, they proposed an AoA estimator which can be readily implemented using adaptive arrays. The estimator requires the knowledge

of the covariance matrix of the element signals in the absence of the desired signal. This requirement can be accommodated in a TDMA system, and consequently the estimator will be further examined in this report under various jamming scenarios.

The estimator involves sum and difference beams,  $w'$  and  $w''$  are analogous to those used in conventional monopulse antennas. The estimator, therefore, will be called the monoestimator. It will be shown that if one has some prior knowledge of the AoA of the desired signal the monoestimator provides an accurate estimate of the AoA (within a fraction of a beamwidth). If however, the expected AoA is not within a half beamwidth of the actual AoA the 'monoestimator' generally breaks down. An alternative estimator is, therefore, proposed in this work. It is also based on the maximum likelihood theory of angle estimation and requires the knowledge of the covariance matrix. But no prior knowledge of the AoA is needed. The new estimator called the 'Q-estimator' can also be implemented using adaptive arrays. It is shown that the Q-estimator provides very accurate estimates of the AoA (within one tenth of a beamwidth) as long as the jammers are outside the main beam of the array. As the angular separation between the desired signal and the jammer decreases, the accuracy of the Q-estimate degrades. However, the estimated AoA still remains within a quarter of a beam width of the true AoA and is therefore adequate for a switched downlink beam of a TDMA system. Furthermore, the Q-estimate can be used as an initial estimate for the monoestimator, further improving the final accuracy for close-in jammers.

In Section 2 the two estimators based on the theory of maximum likelihood estimation are presented. The computer simulation of the two estimators is discussed in Section 3. Some system aspects are also given in this Section. Simulated results are presented and discussed in Section 4. Section 5 contains a summary and conclusions.

## 2. MAXIMUM LIKELIHOOD ESTIMATES OF THE AoA

Maximum Likelihood Methods (MLM) can provide estimates of the directions and strengths of all signals incident on an antenna array. The achievable accuracy of these estimates are indicated by the Cramer-Rao (CR) bound [2]. Maximum Likelihood Procedures come close to achieving the CR bound. El-Behrey, et. al. [3], have shown that the ML estimate virtually attains the CR bound when the signal to noise ratio or the number of antenna elements exceed a given threshold. Similar results were reported by Ksienski and McGhee [4] in a decision theoretic approach to angle estimation.

In this study the covariance of the signals obtained from the antenna elements are used to obtain a Maximum Likelihood estimate of the angle of arrival of the desired signal. Two separate measurements are required to obtain the estimate. One measurement involves the outputs of the antenna elements in the absence of the desired signal but including all corruptive influences such as internally and externally generated noise and directional interfering sources. The other measurement would include the above as well as the desired signal. In a TDMA system these measurements can be accomplished during properly

allocated times. The covariance matrix can be estimated in the period preceeding the time slot during which a request by a new terminal is being made, and the estimation of the AoA will be carried out during the time slot.

Two methods based on the known covariance matrix are presented in this work. In both methods the procedure used to estimate the AoA leads to sum and difference beam patterns, which can be implemented with adaptive receiving array antennas employing a separate control loop for each element [5]. When directional sources are present both the sum and the difference beams have nulls in the directions of the signals included in the covariance matrix. Since the desired signal is excluded from the covariance matrix, the sum beam would not have a null in its direction. Indeed, the weights for the sum beam are chosen to produce maximum signal-to-noise ratio in the steered (desired signal) direction. The null of the difference beam coincides, however, with this direction only when the interference is isotropic.

In the method by Davis, et. al. [1] the likelihood function is expanded around an expected AoA, and the sum beam points to the expected AoA direction. The algorithm or estimator is used to compensate for any bias, i.e. the difference between the expected and the true angle to produce an accurate estimate of the AoA. For the particular case of isotropic noise the estimator acts like an ordinary monopulse system. For this reason the estimator will be called a 'monoestimator'. Just as a monopulse system the monoestimator is accurate if the actual AoA is within a beamwidth of the expected AoA.

In the second method, the global minimum of a Q-function (obtained from the likelihood function) is found. The estimator is called the 'Q-estimator'. The accuracy of the Q-estimator does not depend on an expected AoA, it is limited only by the angular sampling interval used to search for the minimum of the Q-function and by the noise and jamming environment.

In Section 2.1 the likelihood function is derived for a linear array of isotropic elements in the presence of jammers and internal noise. The monoestimator is discussed in Section 2.2. Section 2.3 deals with the Q-estimator. While the following analysis is restricted for simplicity to linear arrays of isotropic elements, the theory and estimators derived here can be readily generalized to arbitrary array geometries of isotropic or directive elements.

### 2.1 The Likelihood Function for a Linear Array of Isotropic Elements

In this section the likelihood function for a linear array of isotropic elements is derived. The derivation is based on the previous work of Davis, et. al. [1]. The system is assumed to be narrowband, consequently the complex envelope of the signal at the output of all array elements may be assumed to be identical. This assumption permits a limited bandwidth without incurring substantial mathematical complications.

Let the array consist of  $L$  elements. A signal arriving at an angle  $\theta$ , measured with respect to broadside, will produce a signal vector  $S(t)$  at the antenna elements, given by



$$S(t) = b V(\epsilon) \quad . \quad (1)$$

where

$$V(\epsilon) = \begin{bmatrix} e^{j \frac{2\pi \rho_1 \epsilon}{\lambda}} \\ e^{j \frac{2\pi \rho_k \epsilon}{\lambda}} \\ \vdots \\ e^{j \frac{2\pi \rho_L \epsilon}{\lambda}} \end{bmatrix} \quad . \quad (2)$$

and  $\rho_k$  = the coordinate of the  $k^{\text{th}}$  element

$\epsilon = \sin \theta$

$\lambda$  = wavelength of the carrier wave

$b$  = complex envelope of the signal at a reference point.

If the signal is contaminated by noise, due to the receiver and external interference, then the total received signal  $X(t)$  is

$$X(t) = S(t) + N(t) \quad . \quad (3)$$

where  $N(t)$  is the received noise vector, given by

$$N(t) = \begin{bmatrix} n_1(t) \\ n_2(t) \\ \vdots \\ n_L(t) \end{bmatrix} \quad . \quad (4)$$

where  $n_i(t)$  is the total noise (internal as well as external) at the  $i^{\text{th}}$  element.

If one assumes that the components of  $N$  are jointly Gaussian, then the probability density for  $N$  can be written as.

$$P(N) = \frac{1}{(\pi)^L} \cdot \frac{1}{|M|} \cdot \exp \{-N^* M^{-1} N\} \quad (5)$$

where  $N^*$  = denotes complex conjugate transpose of  $N$

$M$  = covariance matrix of the element outputs with both internal and external noise but in the absence of the desired signal

$M = E \{N N^*\}$

$|M|$  = the determinant of  $M$

$E\{\cdot\}$  = denotes ensemble average which may be replaced by a time average by invoking the ergodic hypothesis.

From Equations (1) and (3) the probability density for the signal-plus-noise process is

$$P(X/S) = \frac{1}{(\pi)^L} \frac{1}{|M|} \exp \{-[X-bV(\epsilon)]^* M^{-1} [X-bV(\epsilon)]\} \quad (6)$$

The vector  $X$  in Equation (6) is the sampled data set from the  $L$  antenna elements and Equation (6) is the likelihood function. Note that it is a function of  $b$  and  $\epsilon$ . To obtain an estimate of  $\epsilon$  one searches for the values of  $b$  and  $\epsilon$  which maximize the likelihood function. It is convenient to find the maximum of the likelihood function by minimizing the negative of the logarithm of the likelihood function. This is equivalent to minimizing the quadratic form

$$Q(X|b, \epsilon) = [X-bV(\epsilon)]^* M^{-1} [X-bV(\epsilon)] \quad (7)$$

with respect to  $b$  and  $\epsilon$ . In this minimization the covariance matrix  $M$  is assumed to be known or is estimated from data samples. Equation (7) can also be written as

$$Q(X/b, \epsilon) = X^* M^{-1} X - (|X^* M^{-1} V|^2 / V^* M^{-1} V) + V^* M^{-1} V |b - (V^* M^{-1} X / V^* M^{-1} V)|^2. \quad (8)$$

Since the last term in (8) is always positive and real,  $Q$  is minimum for

$$\hat{b} = V^* M^{-1} X / V^* M^{-1} V. \quad (9)$$

The value of  $\hat{b}$  in Equation (9) is the ML estimate of  $b$ . Substituting this value of  $b$  in Equation (8),  $Q(X/b, \epsilon)$  reduces to a function of  $\epsilon$  alone, namely,

$$Q(\epsilon) = X^* M^{-1} X - (|X^* M^{-1} V|^2 / V^* M^{-1} V). \quad (10)$$

The quadratic form in Equation (10) will be called the 'Q-function'. To obtain an estimate of  $\epsilon$  which depends on the data  $X$  and the covariance matrix  $M$  one finds the value of  $\epsilon$  which minimizes the Q-function. One method would be to let

$$\frac{dQ}{d\epsilon} \equiv Q_{\epsilon} = 0 \quad \text{and solve for } \epsilon.$$

$\frac{dQ}{d\epsilon}$  is a transcendental equation in  $\epsilon$  and therefore requires tedious numerical techniques for its solution. Two alternate methods to find  $\epsilon$  which minimize the Q-function are given next. The two methods lead to sum and difference beams, which can be implemented using adaptive arrays, or be obtained by computation.

## 2.2 The Monoestimator

The monoestimator is based on expanding the Q-function around a given angle ("expected AoA"). Let  $\epsilon_1$ , be the expected angle of arrival, then

$$Q(\epsilon) = Q(\epsilon_1) + \left. \frac{dQ}{d\epsilon} \right|_{\epsilon_1} (\epsilon - \epsilon_1) + \frac{1}{2} \left. \frac{d^2Q}{d\epsilon^2} \right|_{\epsilon_1} (\epsilon - \epsilon_1)^2. \quad (11)$$

and,

$$\frac{dQ}{d\epsilon} = \left. \frac{dQ}{d\epsilon} \right|_{\epsilon_1} + \left. \frac{d^2Q}{d\epsilon^2} \right|_{\epsilon_1} \cdot (\epsilon - \epsilon_1). \quad (12)$$

At the minimum,  $\frac{dQ}{d\epsilon} = 0$ . Therefore,

$$\hat{\epsilon} = \epsilon_1 - \frac{Q_{\epsilon} |_{\epsilon_1}}{Q_{\epsilon\epsilon} |_{\epsilon_1}}. \quad (13)$$

where

$$Q_{\epsilon} = \frac{dQ}{d\epsilon} \text{ and } Q_{\epsilon\epsilon} = \frac{d^2Q}{d\epsilon^2}.$$

This estimator was studied by Davis, et. al. [1] and was found to produce rather noisy estimates for the cases considered. It was then modified by replacing the denominator in Equation (13) by an averaged value,  $E\{Q_{\epsilon\epsilon} |_{\epsilon_1}\}$  which resulted in a better performance. The estimator

studied in this work, therefore, is given by

$$\hat{\epsilon} = \epsilon_1 - \frac{Q_{\epsilon} |_{\epsilon_1}}{E\{Q_{\epsilon\epsilon} |_{\epsilon_1}\}}. \quad (14)$$

Assuming that the maximum likelihood estimate of  $b$  is given by Equation (9), Equation (14) can be rewritten [1] to give

$$\epsilon = \epsilon_1 + \frac{b_{11}^2(\Sigma\bar{\Delta} + \Delta\bar{\Sigma}) - \Sigma\bar{\Sigma}(b_{12} + b_{21}) \cdot b_{11}}{2\Sigma\bar{\Sigma}(b_{11}b_{22} - b_{12}b_{21})} \quad (15)$$

where

$$\begin{aligned} b_{11} &= E\{\Sigma\bar{\Sigma}\} = V^*M^{-1}V \\ b_{12} &= E\{\Sigma\bar{\Delta}\} = V^*M^{-1}DV \\ b_{21} &= \bar{b}_{12} \\ b_{22} &= E\{\Delta\bar{\Delta}\} = -V^*DM^{-1}DV \end{aligned} \quad (16)$$

$$D = j \frac{2\pi}{\lambda} \text{diag. } (\rho_1, \rho_2, \dots, \rho_L) \quad (17)$$

$$\Sigma = W_{\Sigma}^* X = V^* M^{-1} X \quad (18)$$

$$\Delta = W_{\Delta}^* X = -V^* D M^{-1} X \quad (19)$$

In above Equations,  $(\bar{\cdot})$  denotes complex conjugate and  $\text{diag}(\rho_k)$  denotes the diagonal matrix with elements  $\rho_k$ . Note that  $\Sigma$  and  $\Delta$  are linear functions of the data  $X$  and  $W_{\Sigma}^*$  is the optimal steady state weight vector of an adaptive array steered to receive signals from the direction defined by vector  $V$  in the presence of interference and noise included in the covariance matrix  $M$ .

If the only noise of the system were receiver noise, then the covariance matrix  $M$  would be proportional to the identity matrix  $I$ .

Under such conditions the present system reduces to a monopulse where,  $\Sigma$  is called a 'sum beam' and  $\Delta$  a 'difference beam'. For this reason  $\Sigma$  and  $\Delta$  in Equations (18) and (19) will be called generalized sum and difference beams, respectively. The weight vectors  $W_{\Sigma}^*$  and  $W_{\Delta}^*$  are such that the two beams form nulls on the interference sources. In the absence of all jammers the difference beam has a null at the peak of the sum beam, but this may not be so for nonisotropic noise or in the presence of interference. The sum and difference beams can be implemented with adaptive array antennas employing a separate control loop for each element. Steering signals for the sum-beam array are  $V(\epsilon_1)$ , i.e., the signals are matched to an incident plane from the angle corresponding to  $\epsilon_1$ . The corresponding steering angles for the difference beam are  $-DV(\epsilon_1)$ . Thus an adaptive array can be used to estimate the AoA of a desired signal in the presence of internal noise as well as interference. The estimate is given by Equation (15) and the estimator is called the 'monoestimator'. The estimation process can, of course, be carried out computationally by sampling the antenna element output signals and computing all the terms in Equation (15).

### 2.3 The Q-Estimator

The monoestimator discussed in Section 2.2 assumes that the AoA is approximately known. If this "expected" value is close (within a fraction of a beamwidth) to the true AoA the final estimate will be quite accurate. If, on the other hand, the expected angle is off by a beamwidth or more the final estimate will be poor. To demonstrate it, one can take the case when only receiver noise is present.

In the absence of all jammers, the covariance matrix,  $M$ , reduces to the identity matrix (assuming that the system noise is normalized such that the receiver noise power at each element is equal to unity) and Equations (16), (17) and (18) yield,

$$\Sigma = V^* X$$

$$\Delta = -V^* D X$$

$$b_{11} = L$$

$$b_{12} = j \sum_{k=1}^L \frac{2\pi\rho_k}{\lambda} = \overline{b}_{21}$$

$$b_{22} = \sum_{k=1}^L \left( \frac{2\pi\rho_k}{\lambda} \right)^2$$

For a symmetrical array centered at  $\rho=0$ ;  $b_{12}=b_{21}=0$  and Equation (15) reduces to

$$\hat{\epsilon} = \epsilon_1 + \frac{L}{b_{22}} \operatorname{Re} \left( \frac{\Delta}{\Sigma} \right) \quad (20)$$

Substituting  $\alpha_k = \frac{2\pi\rho_k}{\lambda} (\sin\theta_s - \sin\theta_1)$ , where  $\theta_s$  is the true AoA of the desired signal and  $\theta_1$  is the expected AoA of the desired signal, Equation (16) yields

$$\hat{\epsilon} = \epsilon_1 + \frac{L}{\sum_k y_k^2} \frac{\sum_k y_k \sin \alpha_k}{\sum_k \cos \alpha_k} \quad (21)$$

$$\text{where } y_k = \frac{2\pi\rho_k}{\lambda}$$

$$\epsilon = \widehat{\sin \theta_s}$$

$$\epsilon_1 = \sin \theta_1 \quad .$$

The expected AoA,  $\theta_1$ , defines the steering angle of the sum beam. If the true AoA,  $\theta_s$ , falls within the main beam of the array, the sign of the correction term in Equation (21) is determined by the sign of  $\theta_s - \theta_1$ . Thus for a small error in the expected value of the AoA, the correction term adjusts the expected value to give a good estimate of the AoA. For large deviation where  $(\theta_s - \theta_1)$  approaches a beamwidth, the individual element contributions no longer add in phase and thus the second term in Equation (21) may no longer provide a correction term even of the correct sign, thus further biasing the estimate. For a good estimate, therefore, the expected value of the AoA in a monoestimator should be within a 3 dB beamwidth of the array.

Such an accurate guess is not very likely with the narrow beamwidths required for the present spot beam SATCOM system. If, however, an AoA estimate accurate to within a fraction of a beam can be obtained by another approach it could provide an input to the monoestimator which would then yield very accurate final AoA's. Such an estimate can be provided by the Q-estimator discussed next.

The Q-estimator can provide adequate estimates on its own, i.e., provide the correct AoA within a quarter of a 3 dB beamwidth and often can do much better. But in very heavy jamming scenarios a combination of both approaches may be preferable and could provide estimates to within an eighth of a 3 dB beamwidth.

To find the AoA, using the Q-estimator, the Q-function (Equation 10) should be minimized. Since it is a function of the direction vector  $V$ , it can be minimized with respect to  $V$ . The vector  $V = V_{min}$  which



minimizes the Q-function will yield the AoA. The Q-function is given by

$$Q(V) = X^*M^{-1}X - |V^*M^{-1}X|^2 / V^*M^{-1}V \quad (22)$$

where

$X = N+S$  (consists of sampled antenna element outputs)

$S$  is the signal vector whose direction vector  $V_s$  is to be estimated.

Note that only the second term in Equation (22) is a function of  $V$ , hence one can minimize the function  $Q_1$  given by,

$$Q_1(V) = V^*M^{-1}V / |V^*M^{-1}X|^2 \quad (23)$$

$$= b_{11} / \Sigma \Sigma \quad (24)$$

Simulation results have shown, however, that the minimum of the Q-function is sharper and thus more easily detectable than that of the  $Q_1$  function. The reason for it appears to be related to the fact that the first term of  $Q$  contains the total signal  $X$  which includes noise components that are also present in the second term. There seems to be a certain amount of compensation provided by the first term to the second term of  $Q$  which  $Q_1$  does not have. This results in less noisy behavior of  $Q$ .

The Q-estimator discussed above involves scanning of the array beam. The angular accuracy of the estimator, therefore will depend upon the scanning step size. To get the minimum, one can proceed as follows.

Let us assume  $Q$  to be a parabolic function of the argument  $\epsilon$  near the minimum ( $\epsilon$  is the direction cosine of the vector  $V$  with respect to the array broadside). Then

$$Q(\epsilon) = Q_0 + a(\epsilon - \hat{\epsilon}_s)^2 \quad (25)$$

where  $Q_0$  is the minimum value of  $Q$ ,  $\hat{\epsilon}_s$  defines the minimum direction cosine and  $a$  is a constant.

$\hat{\epsilon}_s$  can be estimated from three values of  $Q$  which are used to eliminate  $Q_0$  and  $a$ . Let the value of the  $Q$ -function be known for  $\epsilon_1$ ,  $\epsilon_2$ , and  $\epsilon_3$  and assume that  $Q(\epsilon_2)$  is the smallest of the three, then

$$\hat{\epsilon}_s = \epsilon_2 + \frac{\Delta\epsilon}{2} \frac{Q(\epsilon_3) - Q(\epsilon_1)}{2Q(\epsilon_2) - [Q(\epsilon_1) + Q(\epsilon_3)]} \quad (26)$$

where  $\Delta\epsilon = \epsilon_3 - \epsilon_2 = \epsilon_2 - \epsilon_1 > 0$

A note of caution, however, is appropriate at this point regarding the ultimate accuracy of the estimate. The  $Q$ -function is noisy even with ideal signal processing, since it depends on samples from noisy sources. In an actual implementation, quantization noise from AD converters and errors due to digital computations would also contribute. These errors are not included here, but will affect the final accuracy of an implemented system. To reduce the various noise effects it is anticipated that the  $Q$ -function will have to be averaged over a number of samples. In a practical system the number of samples averaged will have to be kept small, however, to minimize complexity and time delay.

In the next two sections simulation results using two estimates will be presented. The AoA will be estimated for different interference scenarios.

### 3. SYSTEM ASPECTS AND SIMULATION

A computer model for the simulation of the monoestimator and the Q-estimator was developed. The estimation procedures involve two steps. In the first step the covariance matrix is calculated from the element signals. At this step internal and external noise sources and interference are included but no desired signal is assumed to be present. In the second step the AoA of the desired signal is estimated from the sampled element signals with all sources including the desired signal assumed present. Since the results depend on the simulation model and noise generators, the model will be discussed in detail.

The simulation model is discussed in Section 3.1. Since the system of interest is a satellite based TDMA system, the system aspects are given in Section 3.2. Section 3.3 contains basic assumptions.

#### 3.1 The Simulation Model

##### a) Generation of the antenna element signals

Three different types of signals are assumed to be incident on the array elements: Gaussian nonisotropic (directive) noise, CW interferences and a CW desired signal. Receiver noise is also present.

The internal noise is independently generated for each element. The complex noise voltage is assumed to have a Rayleigh amplitude distribution and uniform phase with average power of unity. The noise voltages can, therefore, be represented by

$$n = g_1 + jg_2 \quad . \quad (27)$$

where  $g_1$  and  $g_2$  have normal distributions [ $\mu=0$ ,  $\sigma=1$ ]. The same model is used to generate the voltage from Gaussian nonisotropic noise (noise type jamming sources) of power  $P_J$ . The voltage due to one of these jammers, at the reference element, is given by

$$n_i = \sqrt{P_J} (g_{i1} + jg_{i2}) \quad . \quad (28)$$

The voltages at the other elements are

$$n_{ik} = n_i \exp \left[ j \frac{2\pi}{\lambda} \epsilon_i (\rho_k - \rho_r) \right] \quad (29)$$

where  $\epsilon_i$  defines the direction of the jammer and  $\rho_r$  is the location of the reference element.

The CW signals incident on the array are assumed to have a constant envelope but a randomly varying phase for successive time samples as seen at the reference element. The voltage at the reference element due to a CW signal is, therefore, given by

$$n_{CW} = \sqrt{P_{CW}} \exp (j2\pi n) \quad (30)$$

where  $n$  is uniformly distributed over the interval  $[0,1]$ . The voltages at the other array elements due to this CW signal, therefore are

$$n_{CW k} = n_{CW} \exp \left( \frac{j2\pi}{\lambda} \epsilon_{CW} (\rho_k - \rho_r) \right) \quad (31)$$

where  $\epsilon_{CW}$  defines the direction of the CW signal.

b) Generation of the covariance matrix

The elements of the covariance matrix are given by

$$m_{\ell j} = E\{x_{\ell} x_j\} \quad . \quad (32)$$

where  $x_{\ell}$  =  $\ell^{\text{th}}$  element signal and  $E\{\cdot\}$  denotes ensemble average. For an ergodic process the ensemble average is equal to the time average. Two separate methods to compute the covariance matrix are given. The first one, which assumes a 'known' covariance matrix, does not use randomly generated element signals but assumes the interference scenario to be known. In this case,

$$m_{\ell i} = \sum_{k=1}^{N_J} P_{Jk} \exp[j(\phi_{ik} - \phi_{\ell k})] + \delta_{\ell i} \quad . \quad (33)$$

where  $N_J$  is the total number of jammers,

$P_{Jk}$  is the  $k^{\text{th}}$  jammer power (normalized to receiver noise),

$\phi_{ik}$  is the  $k^{\text{th}}$  jammer phase at the  $i^{\text{th}}$  element measured with respect to reference element,

$\delta_{\ell i}$  is the Kronecker delta.

In the second method the sampled element signals are used to calculate the covariance matrix elements. This leads to the "unknown" or estimated covariance matrix. The desired signal is assumed to be absent while the sampling of the elements is being carried out. The estimated covariance matrix elements are given by

$$m_{\ell i} = \frac{1}{N_S} \sum_{k=1}^{N_S} \bar{x}_{\ell k} x_{ik} \quad . \quad (34)$$

where  $N_S$  is the number of the independent time samples used for averaging.

This estimate of the covariance matrix gives the maximum likelihood estimate of  $M$  and will be denoted by  $\hat{M}$ .

### c) Angle of Arrival Estimation

The monoestimate and the Q-estimate of the AoA are found by using the sampled antenna element signals generated during the time slot when the desired signal is assumed to be present. While calculating the correction factor for the monoestimator and the Q-function for the Q-estimator an average over a number of samples is taken. The accuracy of the estimate depends on the number of samples used. It is, of course, desirable to keep the total number of samples as low as possible to minimize the computational burden and time delay. Results for different number of samples will be given in Section 4.

## 3.2 System Aspects

The values of the parameters chosen in the simulation are appropriate to a SATCOM system which uses a spot beam pointing, at any direction within the earth field of view, an approximately  $17^\circ \times 17^\circ$  cone from a synchronous orbit.

The antenna element patterns must, therefore, cover the earth field of view. If the array elements have a beamwidth of  $20^\circ \times 20^\circ$ , the resulting element directivity is about 20 dB. The element beamwidth of  $20^\circ$  requires an element aperture of about  $2.5\lambda$ . This also means that an

inter-element distance of at least  $2.5\lambda$  is necessary. Assuming that a spot beam of  $1^\circ$  is required (3db beamwidth) the required aperture diameter would be approximately  $50\lambda$ . The corresponding aperture size would be  $250\lambda$  if  $0.2^\circ$  spot beam is required. For a linear array the number of elements would be 20 and 100, respectively.

The AoA estimator should use as few of the array elements as possible (to increase the speed). The total number of elements required for AoA estimation depends on the specific system requirements for angular resolution and the necessary accuracy of the AoA estimate. It is also affected by the number of jammers (the total number of elements should exceed the total number of jammers). The simulation results using five and ten elements are given in Section 4. The jammer scenarios include one and two jammers.

Following is a sample calculation of the received signal-power per element and the signal to noise ratio at the output of the array elements,

Earth Terminal (assuming a small mobile terminal): Transmitted power = 1 KW at X-band from a 2 meter diameter antenna, gives a PG-product of  $\approx 76$  dBW.

Transmission loss: Atmosphere  $\approx 3$  dB and propagation over 40,000 is approximately 163 dB.

Satellite array element: Element loss  $\approx 3$  dB.

Receiver: A noise figure of 3 dB gives an equivalent noise power of -141 dBW/MHz of receiver bandwidth for a noise temperature of  $300^\circ$  K.

The resulting signal-to-noise-ratio is then 28 dB for a 1 MHz receiver bandwidth. For a 10 MHz bandwidth, the estimated received

signal-to-noise ratio is about 15-20 dB per element. Most results are for 10 dB signal-to-noise ratio, thus providing some margin.

As discussed before, the desired signal should not be present when estimating the covariance matrix. In a TDMA system, either silent time slots should be scheduled in the time frame, or to increase throughput the covariance matrix can be updated during the transmission of a current terminal and the angle estimation carried out during the following "listening" slot. This would cost at most an additional null in the direction of the previous transmitter.

### 3.3 Assumptions in the Simulation

The covariance matrix is simulated by two different methods. One assumes that the covariance matrix is known a priori and the other estimates the matrix by sampling the antenna elements and carrying out the correlation. In the case of a known covariance matrix the receiver noise voltages at each of the array elements are assumed to be uncorrelated with each other and with the incident signals. Further, the incident desired signal and the jammers are assumed to be uncorrelated. These assumptions lead to a positive definite covariance matrix.

The estimated covariance matrix is calculated using sample antenna element signals. The element signals due to each incident source are assumed to be correlated while the signals due to receiver noise are assumed to be uncorrelated. Further, element signals due to different incident sources are assumed to be uncorrelated.



All the incident signals on the array are assumed to be CW signals of the same frequency. The covariance matrix is assumed to include all the jammers but not the desired signal.

In practical systems quantization noise from A/D convertors and digital computation may contribute to performance degradation, but these are not considered in the simulation. The only noise present, therefore, is contained in the sample element signal vector  $X$  discussed and defined above. To reduce this noise the results are averaged over a number of samples. In a practical system the total number of samples should be kept small.

Finally, the array is assumed to have enough degrees of freedom to null all the jammers.

#### 4. SIMULATED RESULTS AND DISCUSSION

In this section some typical estimates of the AoA using a simulated monoestimator and a Q-estimator are presented. The estimator using the Q-function (Equation (22)) provides better results than using the  $Q_1$  function (Equation (23)) and consequently the Q-function is used in most of the results to be shown. Sum and difference patterns are also presented for the purpose of illustration. The AoA is estimated for several scenarios, namely in the absence of all jammers, in the presence of a single jammer and in the presence of two jammers.

Section 4.1 contains the result using the known covariance matrix. The estimates using the estimated covariance matrix are given in Section 4.2

#### 4.1 Known Covariance Matrix

##### a) AoA Estimation in the Absence of all Jammers

Figure 1 shows the estimated AoA,  $\hat{\theta}_{\text{mono}}$ , using the monoestimator, as a function of the difference between the expected AoA and the true AoA in the absence of jammers. The estimated AoA is given for different input signal-to-noise ratios denoted as  $P_s$  and given in terms of db over noise or dBN. Note that for a good estimate the expected angle should be within half a beamwidth from the true AoA. The resulting accuracy is then within one tenth of the beamwidth of the array. If the expected AoA is within a quarter of the beamwidth the resulting accuracy is better than 3 percent of the beamwidth. In the above computation the results were averaged over 100 samples. If a smaller number of samples is used a larger input signal-to-noise ratio is needed to achieve the same accuracy in the estimate of the AoA. For example, for an average of 10-20 samples a minimum of 5 dB  $P_s/N$  is required. At 0 dBN the accuracy degrades to about a quarter of a beamwidth.

Figure 2 shows a plot of the Q-function versus  $(\theta - \theta_s)$  the difference between the scan angle  $\theta$  and the true angle  $\theta_s$  for different values of  $P_s$ . The angular sampling is at quarter of a beamwidth intervals and the results are averaged over ten sampling sets. Note that the estimated AoA (minimum of the Q-function) is very accurate for  $P_s$  as low as 0dBN. The accuracy is within 2 percent of the beamwidth. If the angular sampling rate is decreased to one beamwidth the performance degrades, but it was found that the Q-estimator is not as sensitive to the number of time samples as the monoestimator.

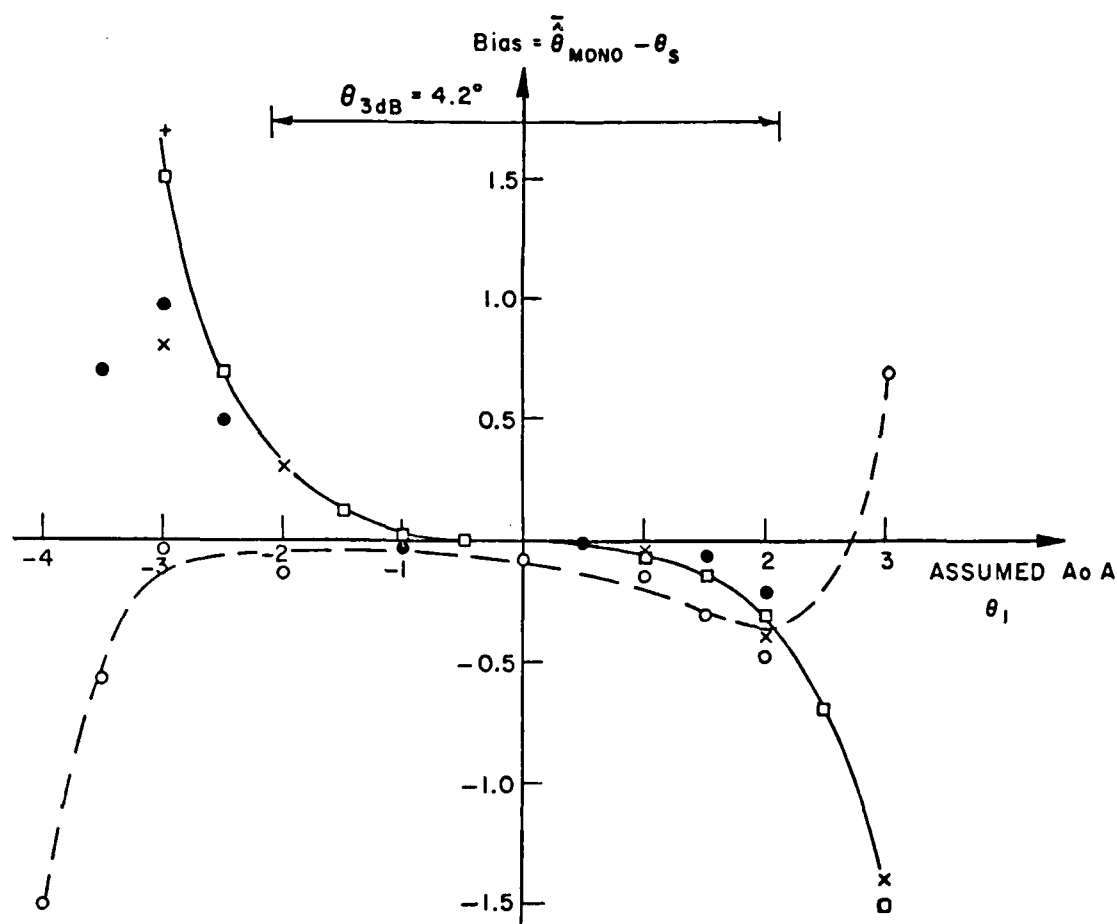


Figure 1. Estimated AoA as a function of the assumed AoA for the monoestimator. Average over 100 samples. Array 3 dB-beamwidth  $\theta_{3dB}=4.2^\circ$  with 5 or 10 elements. True AoA of the desired signal  $\theta_s=0^\circ$ . No Jamming.

o  $P_s = 0$  dBN/5 elements

•  $P_s = 0$  dBN/10 elements

x  $P_s = 5$  dBN/5 elements

+  $P_s = 10$  dBN/5 elements

□  $P_s = 20$  dBN/5 elements

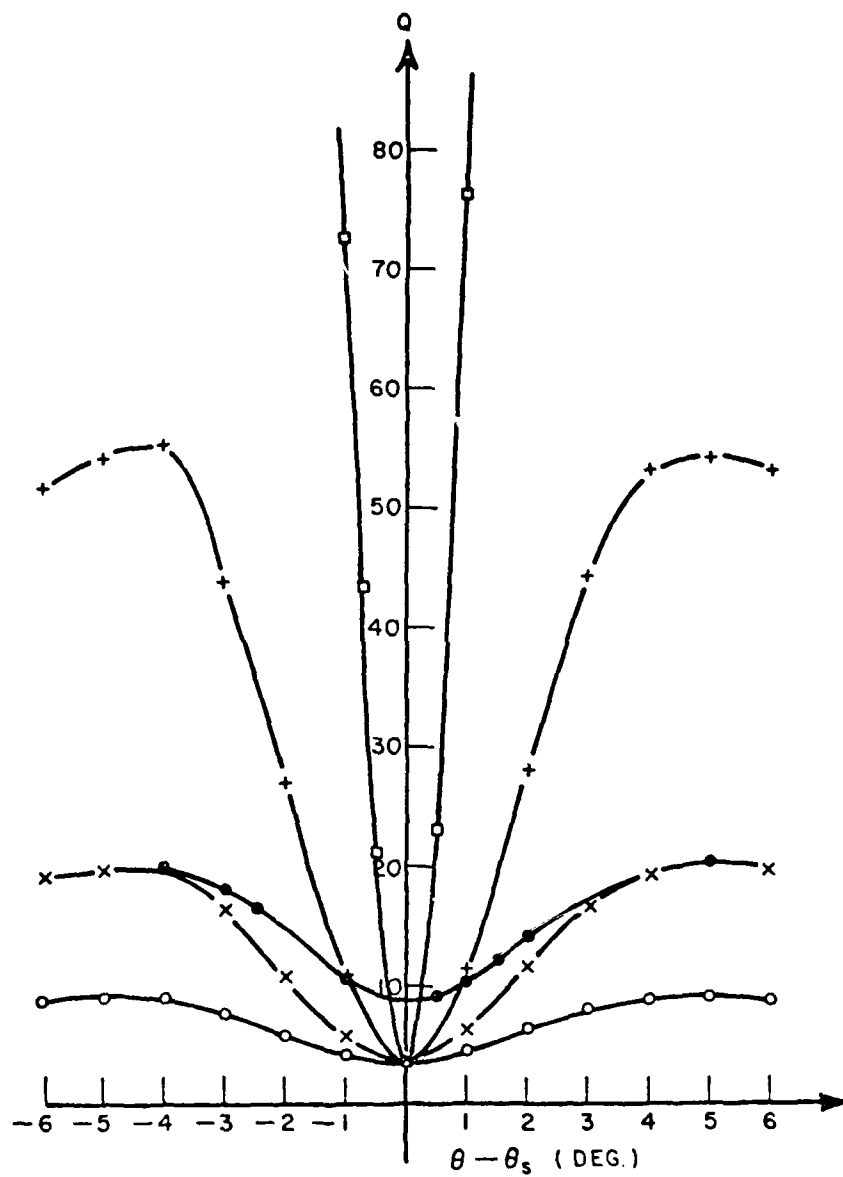


Figure 2. Q-function versus  $(\theta - \theta_s)$ . Averaged over 10 samples.

No jamming. Curve parameters same as for Figure 1.

Doubling the number of elements while keeping the beamwidth constant does not affect the estimation accuracy.

b) AoA Estimation in the Presence of One Jammer

Figure 3 shows the bias in the estimated AoA for both the monoestimator (with expected AoA of  $-2^\circ$ ,  $-0.4^\circ$  and  $1.2^\circ$  respectively) and for the Q-estimator (using angular sampling rates of  $1.6^\circ$  and  $0.2^\circ$ ) as a function of the angular displacement between the AoA of the desired signal and the jammer. The array consists of five elements spaced  $2.5\lambda$  apart and has a beamwidth of  $4.2^\circ$ . Both signals are 10 dB stronger than the receiver noise at each element.

For the monoestimator, if the expected AoA is close to the true AoA, and is not between the jammer and signal direction, good estimates result even for small angular separation between the signal and the jammer. Indeed the estimate is as close as  $0.1^\circ$  or about 3 percent of beamwidth. For large discrepancies between the true AoA and the expected AoA the monoestimator seems to breakdown when the jammer approaches the desired signal to within a quarter of beamwidth. Also, when the expected AoA is closer to the jammer than to the desired signal the estimate is less reliable.

The estimated AoA's obtained using the Q-estimator for a sampling density of  $1.6^\circ$  or .4 beamwidths are good as long as the angular separation between the desired signal and the jammer is fairly large. Although the estimates degrade as the jammer approaches the desired signal the degradation is graceful and the estimate still provides a fairly good indication (within a quarter of a beamwidth) of the location

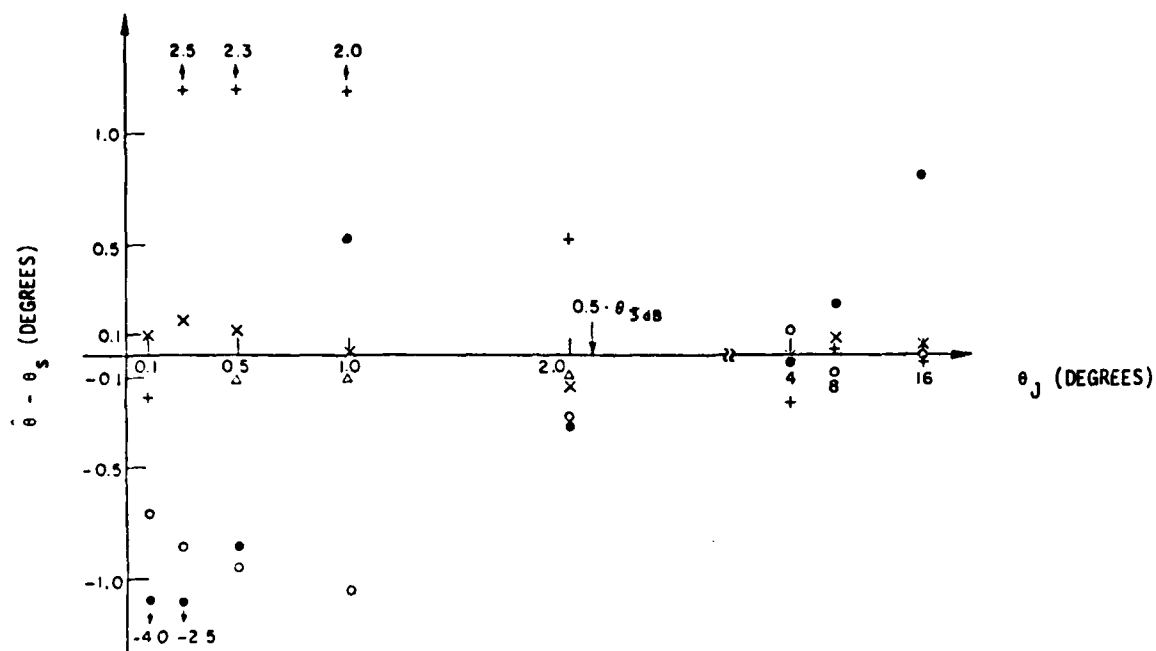


Figure 3. Estimated AoA using a 5 element array, spaced  $2.5\lambda$  apart as a function of the angular distance between one jammer at  $\theta_j$  and the desired signal at  $\theta_s=0^\circ$ . Averaged over 20 samples.

Signal power  $P_s=10$  dBN

Jammer power  $P_j=10$  dBN

•  $\hat{\theta}_{\text{Mono}}$  resulting from expected AoA of  $-2.0^\circ$

x  $\hat{\theta}_{\text{Mono}}$  resulting from expected AoA of  $-0.4^\circ$

+  $\hat{\theta}_{\text{Mono}}$  resulting from expected AoA of  $+1.2^\circ$

o  $\hat{\theta}_Q$  for angular sampling density of  $1.6^\circ$

$\Delta$   $\hat{\theta}_Q$  for angular sampling density of  $0.2^\circ$ ,

Q-values averaged over 10 time samples.

of the desired signal, and would provide a good "expected" angle for the monoestimator. To further improve the Q-estimate a higher sampling density can be used resulting in excellent accuracy. For a sampling density of  $0.2^\circ$  the estimate is within  $0.1^\circ$  (.025 of a beamwidth), or half the intersample distance.

An added advantage of the Q-estimator is the insight provided into the reliability of the estimate which is gained in the process of computing the values of Q at the different scan or sample angles. One can observe whether there is smooth convergence to the minimum or an erratic behavior. Also it is rather apparent when there is a need for closer sampling. This compares to just a number obtained from the monoestimate which gives no hint as to its quality. One could, of course, in principle compute the variance of the estimate if a statistically sufficient number of samples and computation time were available.

Figure 4 shows the estimated AoA when the number of elements is increased to ten while keeping the beamwidth constant. There is no significant improvement in the performance of the two estimators. In the following discussion, therefore, only the 5-element array will be considered.

In Figures 5 and 6 the jammer power is increased to 30 dB and 50 dB respectively. The monoestimator performance is improved a little, in that the jammer can be moved closer to the desired signal. However, the Q-estimator seems to fail when the angular separation between the jammer and the desired signal approaches a tenth of the beamwidth. This

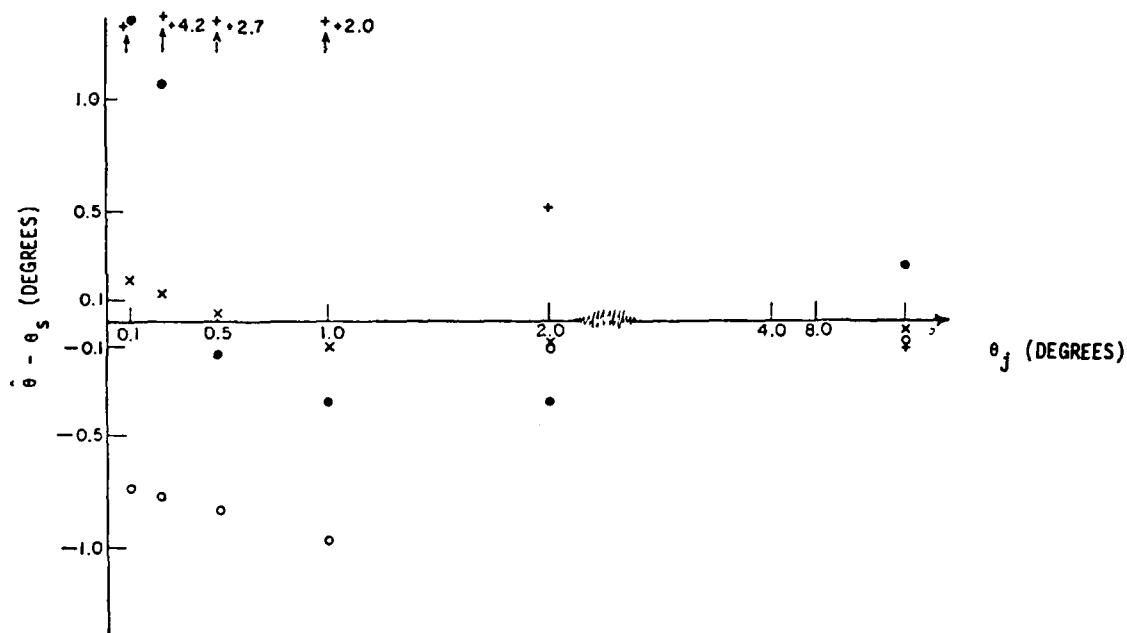


Figure 4. Estimated AoA using a 10 element array spaced  $1.25\lambda$  apart as a function of the angular distance between one jammer at  $\theta_j$  and the desired signal at  $\theta_s=0^\circ$ . Averaged over 20 samples.

Signal power  $P_s=10$  dBN

Jammer power  $P_j=10$  dBN

●  $\hat{\theta}_{Mono}$  resulting from expected AoA of  $-2.0^\circ$

x  $\hat{\theta}_{Mono}$  resulting from expected AoA of  $-0.4^\circ$

+  $\hat{\theta}_{Mono}$  resulting from expected AoA of  $+1.2^\circ$

o  $\hat{\theta}_Q$  for angular sampling density of  $1.6^\circ$

Q-values averaged over 10 time samples.



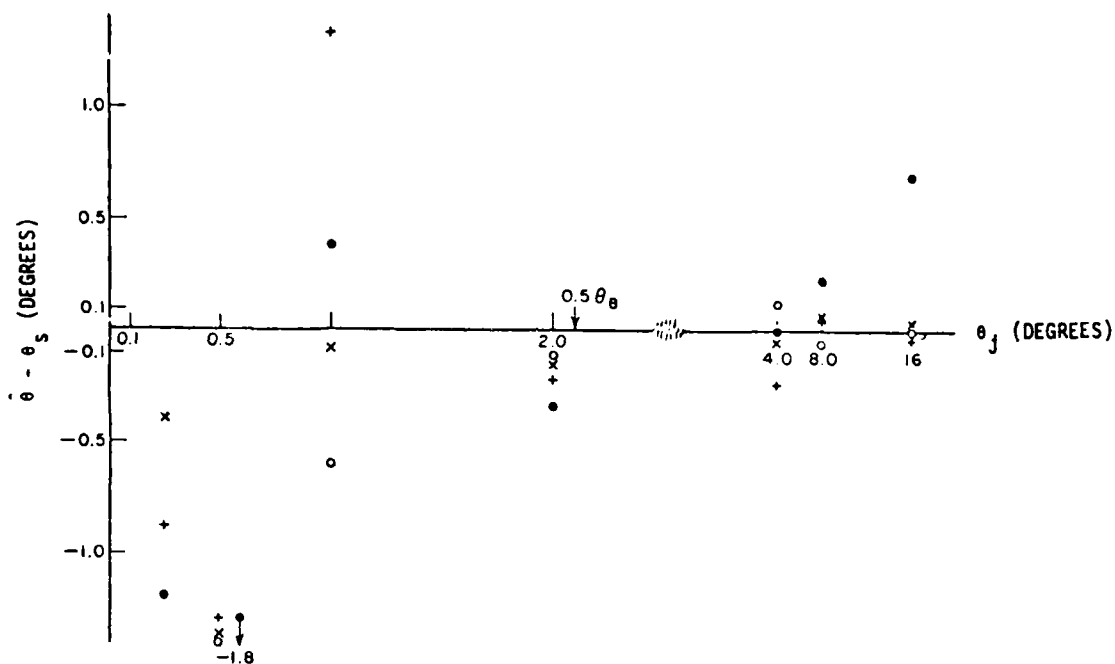


Figure 5. Estimated AoA using a 5 element array as a function of the angular distance between one jammer at  $\theta_j$  and the desired signal at  $\theta_s=0^\circ$ . Averaged over 20 samples.

Signal power  $P_s=10$  dBm

Jammer power  $P_j=30$  dBm

•  $\hat{\theta}_{\text{Mono}}$  resulting from expected AoA of  $-2.0^\circ$

x  $\hat{\theta}_{\text{Mono}}$  resulting from expected AoA of  $-0.4^\circ$

+  $\hat{\theta}_{\text{Mono}}$  resulting from expected AoA of  $+1.2^\circ$

o  $\hat{\theta}_Q$  for angular sampling density of  $1.6^\circ$

Q-values averaged over 10 time samples.

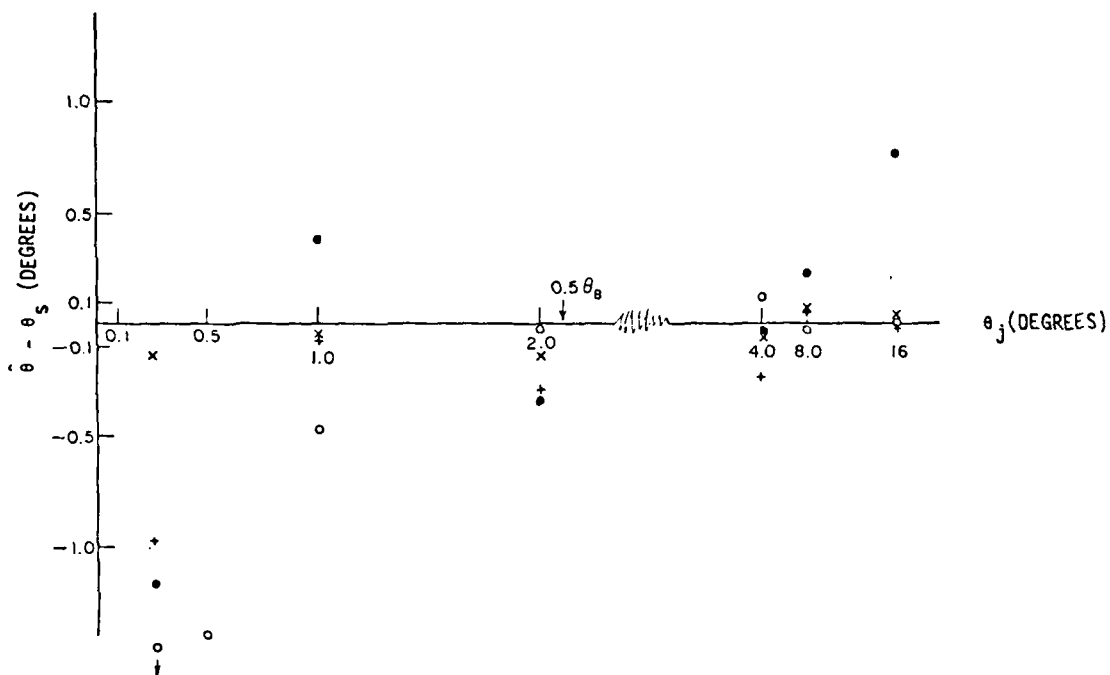


Figure 6. Estimated AoA using a 5 element array as a function of the angular distance between one jammer at  $\theta_j$  and the desired signal at  $\theta_s=0^\circ$ . Averaged over 20 samples.

Signal power  $P_s=10$  dBN

Jammer power  $P_j=50$  dBN

•  $\hat{\theta}_{\text{Mono}}$  resulting from expected AoA of  $-2.0^\circ$

x  $\hat{\theta}_{\text{Mono}}$  resulting from expected AoA of  $-0.4^\circ$

+  $\hat{\theta}_{\text{Mono}}$  resulting from expected AoA of  $+1.2^\circ$

o  $\hat{\theta}_Q$  for angular sampling density of  $1.6^\circ$

Q-values averaged over 10 time samples.

effect can be seen in more detail in Figure 7, which shows the Q-function plotted as a function of steering direction. Note that for a large difference between the jammer power and the signal power the Q-function is quite flat and the minimum is displaced by several degrees from the true AoA.

Note that the Q-estimates are consistently biased away from the jammer, i.e.,  $\theta_Q$  is negative while the jammer location  $\theta_j$  is positive. It is thus apparent that the Q-estimate would provide the right bias in the expected AoA for the optimum performance of the monoestimator. Indeed using the Q-estimate as an input to the monoestimator yields excellent results. This is shown in the legend of Figure 7 by  $\rightarrow \theta_{Mono}$ . Thus the first line indicates a three-fold improvement for  $\theta_j = 2^\circ$  where  $\hat{\theta}_Q = 0.29^\circ$  leads to  $\hat{\theta}_{Mono} = 0.1^\circ$ . The improvement is even larger for high jammer powers and  $\theta_j = 1^\circ$ , resulting in  $\hat{\theta}_Q = -1^\circ \rightarrow \hat{\theta}_{Mono} = 0.2^\circ$ .

When the signal power is increased to the same level as the jammer power (30 dB), the accuracy of the Q-estimator improves (Figure 8). The monoestimator, though, still gives estimates which are sensitive to the jammer scenario, yet the accuracy is better than in the previous scenarios. The sum patterns and the difference patterns are helpful in understanding the performance of the monoestimator and are discussed in the following pages.

Figures 9-15 show the adapted sum and difference patterns for various jammer scenarios and expected AoA's. In Figures 9 and 10 the angular separation between the jammer and the expected AoA is more than a beamwidth ( $BW = 4.2^\circ$ ,  $\theta_j \sim 16^\circ$ ). Note that sum and difference patterns

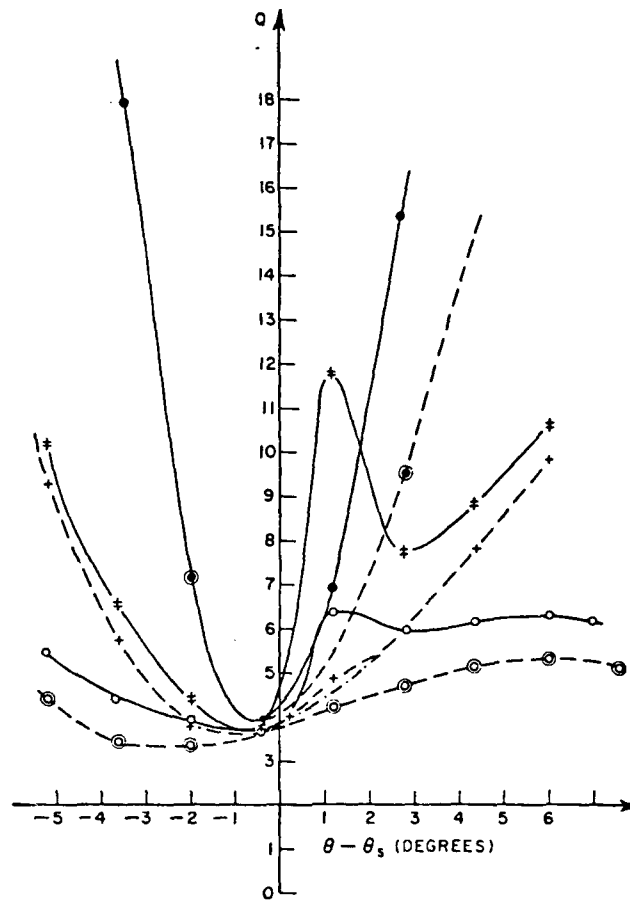


Figure 7. Plots of Q-function, averaged over 10 samples, for different scenarios. 5 element array ( $\theta_3$  dB=4.2°). Desired signal power  $P_S=10$  dBN, true AoA  $\theta_S=0^\circ$ .

Angular sampling density  $1.6^\circ$  for  $\hat{\theta}_Q$ .

●  $P_j=10$  dBN,  $\theta_j=2^\circ$  gives  $\hat{\theta}_Q=-.29^\circ \rightarrow \hat{\theta}_{\text{Mono}}=0.1^\circ$

×  $P_j=10$  dBN,  $\theta_j=1^\circ$  gives  $\hat{\theta}_Q=-1.0^\circ \rightarrow \hat{\theta}_{\text{Mono}}=0.5^\circ$

○  $P_j=10$  dBN,  $\theta_j=5^\circ$  gives  $\hat{\theta}_Q=-1.0^\circ \rightarrow \hat{\theta}_{\text{Mono}}=0.5^\circ$

⊖  $P_j=30$  dBN or 50 dBN,  $\theta_j=2$  gives  $\hat{\theta}_Q=-0.15^\circ \rightarrow \hat{\theta}_{\text{Mono}}=0.15^\circ$

+  $P_j=30$  dBN or 50 dBN (---),  $\theta_j=1^\circ$  gives  $\hat{\theta}_Q=-1^\circ \rightarrow \hat{\theta}_{\text{Mono}}=0.2^\circ$

$\theta_j=0.3^\circ$  gives  $\hat{\theta}_Q=-0.4^\circ \rightarrow \hat{\theta}_{\text{Mono}}=0.15^\circ$ .

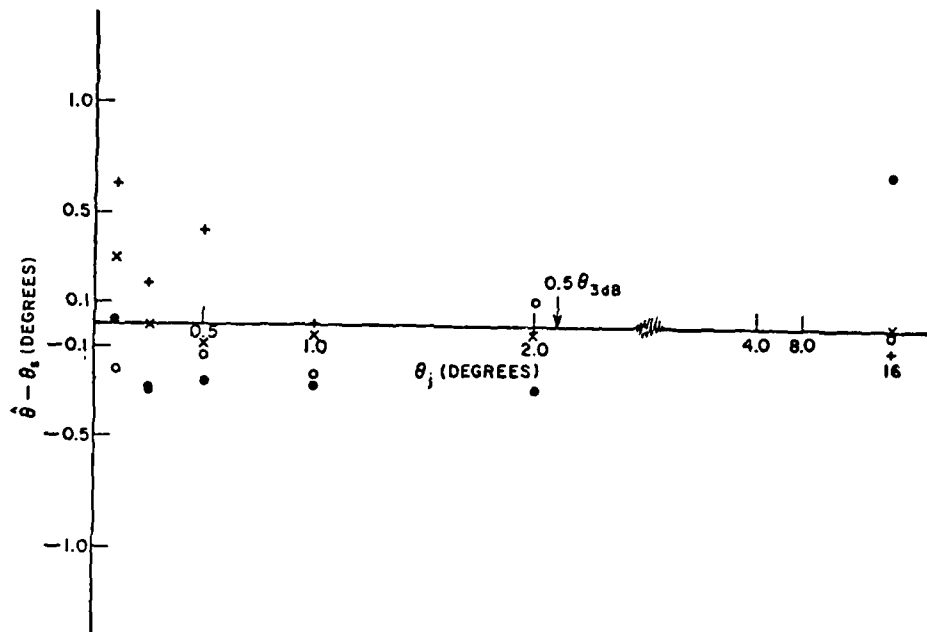


Figure 8. Estimated AoA using a 5 element array as a function of the angular distance between one jammer at  $\theta_j$  and the desired signal at  $\theta_s=0^\circ$ . Averaged over 20 samples.

Signal power  $P_s=30$  dBN

Jammer power  $P_j=30$  dBN

•  $\hat{\theta}_{Mono}$  resulting from expected AoA of  $-2^\circ$

x  $\hat{\theta}_{Mono}$  resulting from expected AoA of  $-0.4^\circ$

+  $\hat{\theta}_{Mono}$  resulting from expected AoA of  $+1.2^\circ$

o  $\hat{\theta}_Q$  for angular sampling density of  $1.6^\circ$

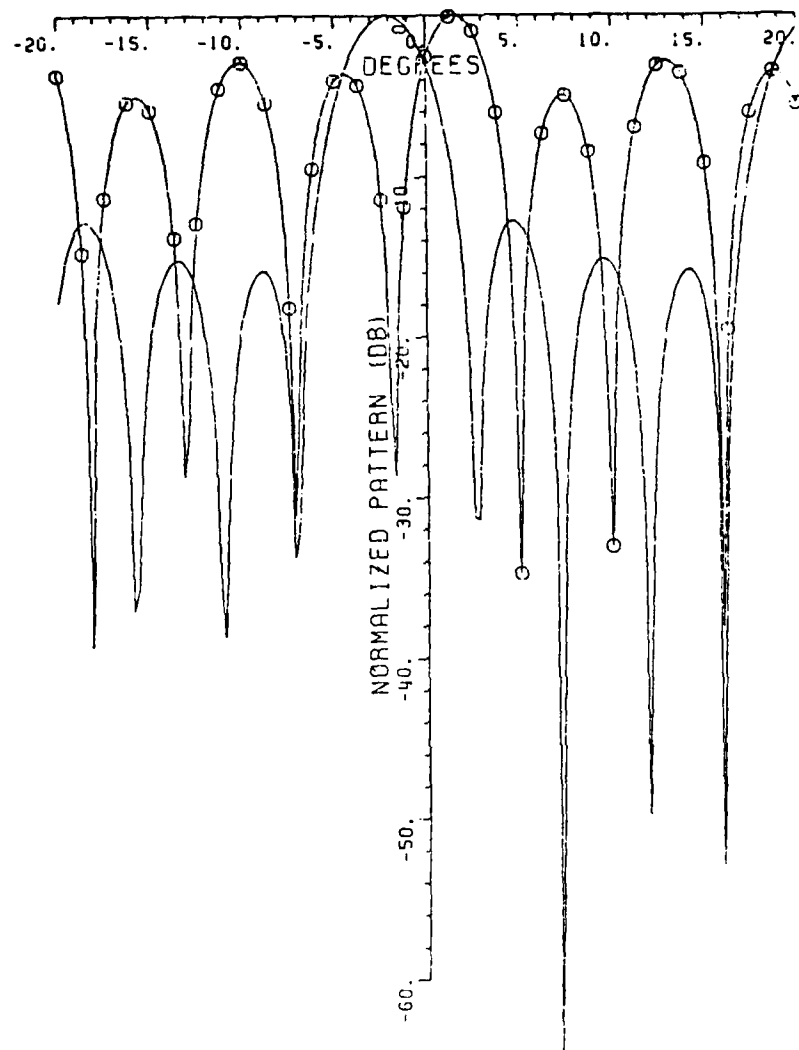


Figure 9. Sum and difference patterns for a 5 element array with inter-element spacing  $2.5\lambda$ . The sum pattern is represented by a solid line, the difference pattern is denoted by a solid line drawn through circles for which the values were computed.

Steering angle  $\theta_{\text{exp}} = -2^\circ$

Jammer with power  $P_j = 10$  dBN at  $\theta_j = 16^\circ$

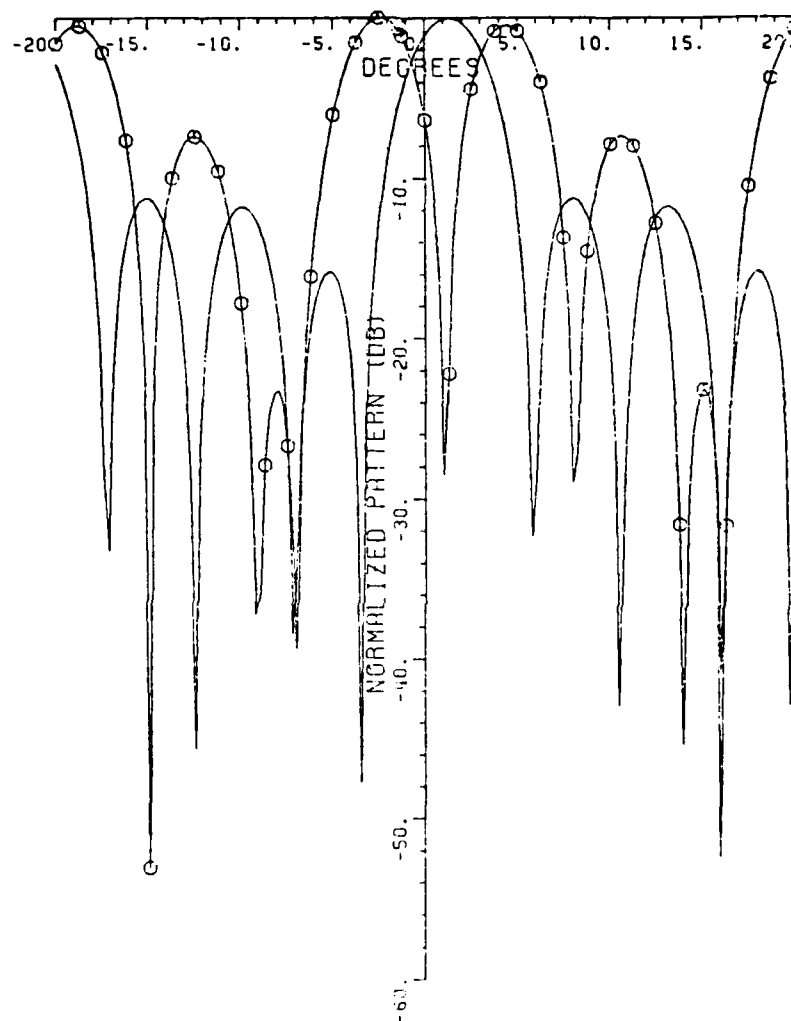


Figure 10. Sum and difference patterns for 5 element array with  
inter-element spacing  $2.5\lambda$ .  
Steering angle  $\theta_{\text{exp}}=1.2^\circ$   
Jammer with power  $P_j=10$  dBN at  $\theta_j=16^\circ$

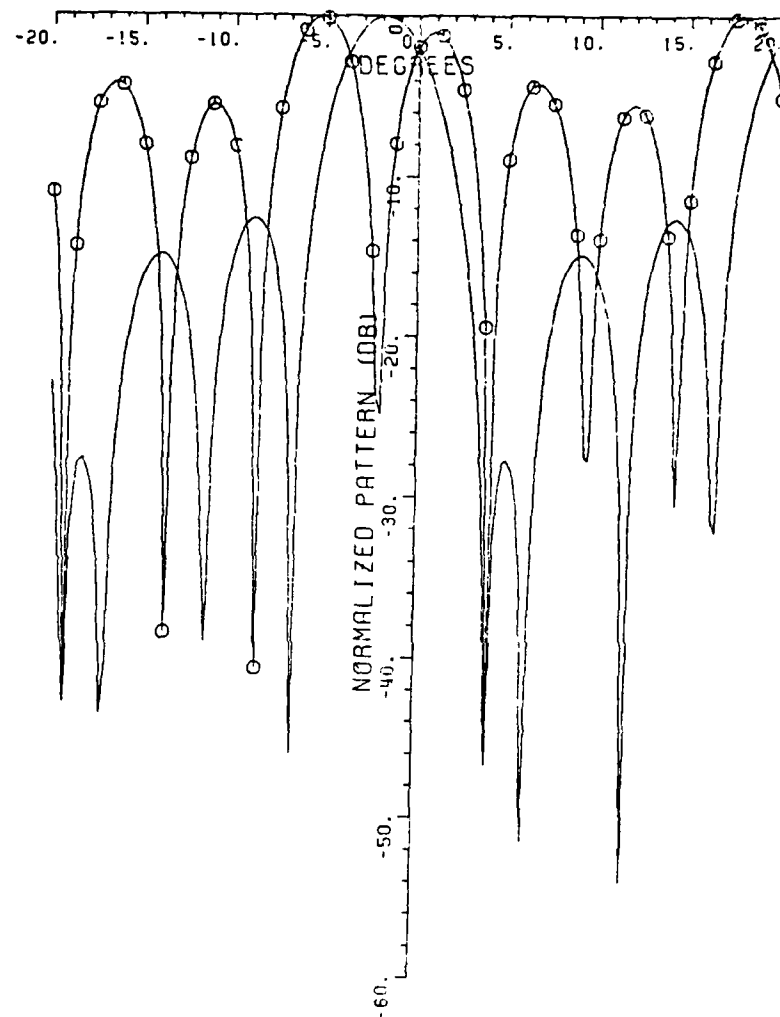


Figure 11. Sum and difference patterns for 5 element array with  
inter-element spacing  $2.5\lambda$ .

Steering angle  $\theta_{\text{exp}} = -2^\circ$

Jammer with power  $P_j = 10$  dBN at  $\theta_j = 4^\circ$



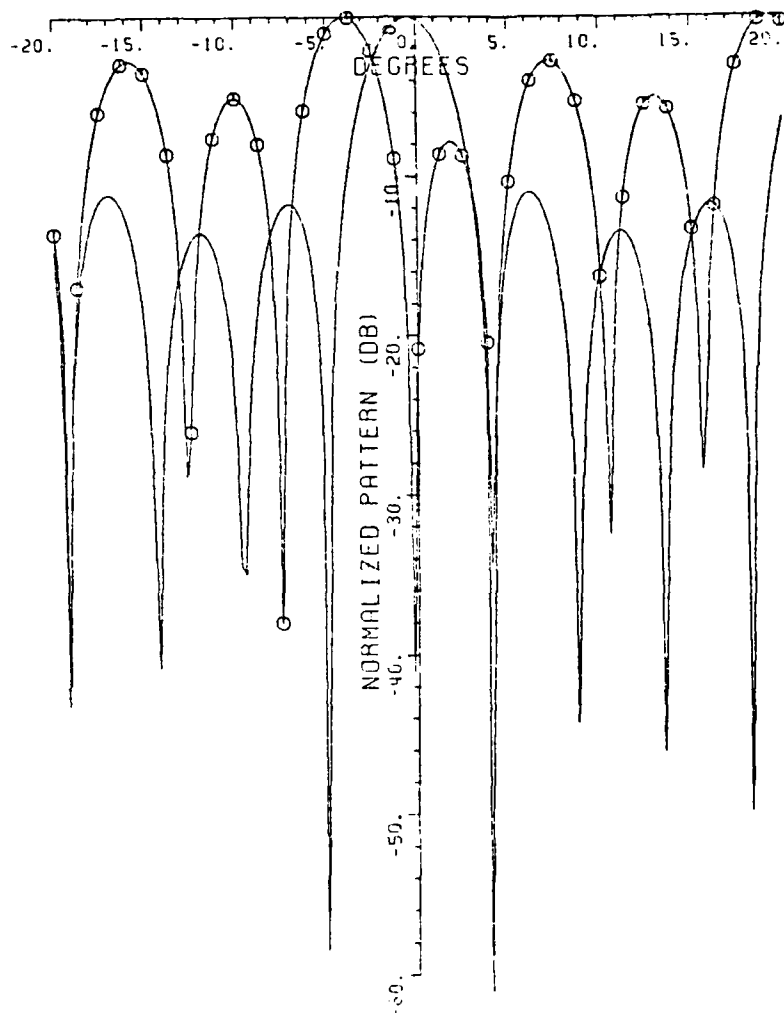


Figure 12. Sum and difference patterns for 5 element array with  
inter-element spacing  $2.5\lambda$ .

Steering angle  $\theta_{exp} = -0.4^\circ$

Jammer with power  $P_j = 10$  dBN at  $\theta_j = 4^\circ$

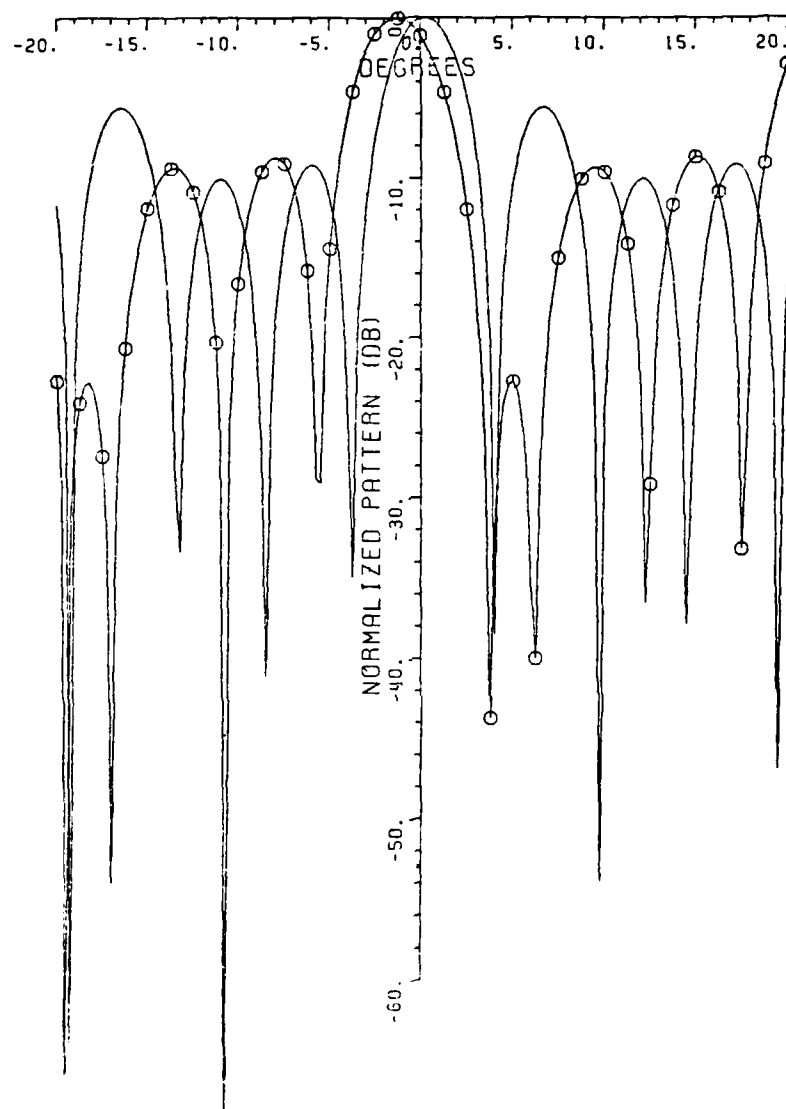


Figure 13. Sum and difference patterns for 5 element array with  
inter-element spacing  $2.5\lambda$ .  
Steering angle  $\theta_{\text{exp}} = +1.2^\circ$   
Jammer with power  $P_j = 10$  dBN at  $\theta_j = 4^\circ$

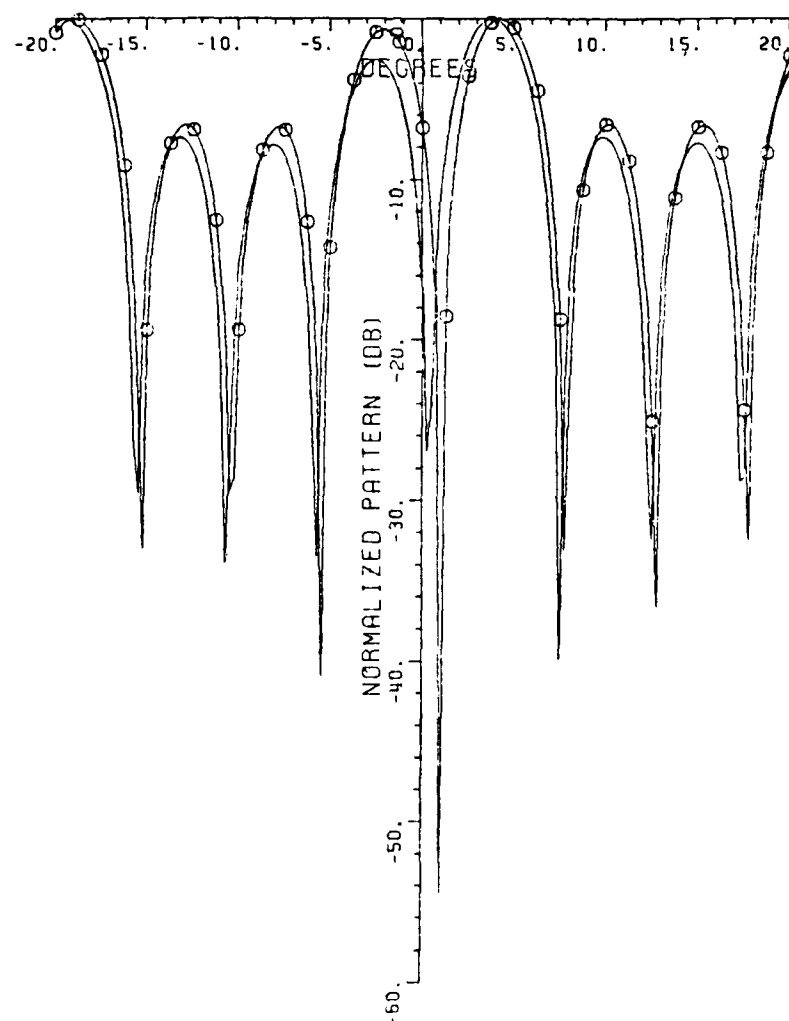


Figure 14. Sum and difference patterns for 5 element array with  
inter-element spacing  $2.5\lambda$ .

Steering angle  $\theta_{\text{exp}}=1.2^\circ$

Jammer with power  $P_j=10$  dBN at  $\theta_j=1^\circ$

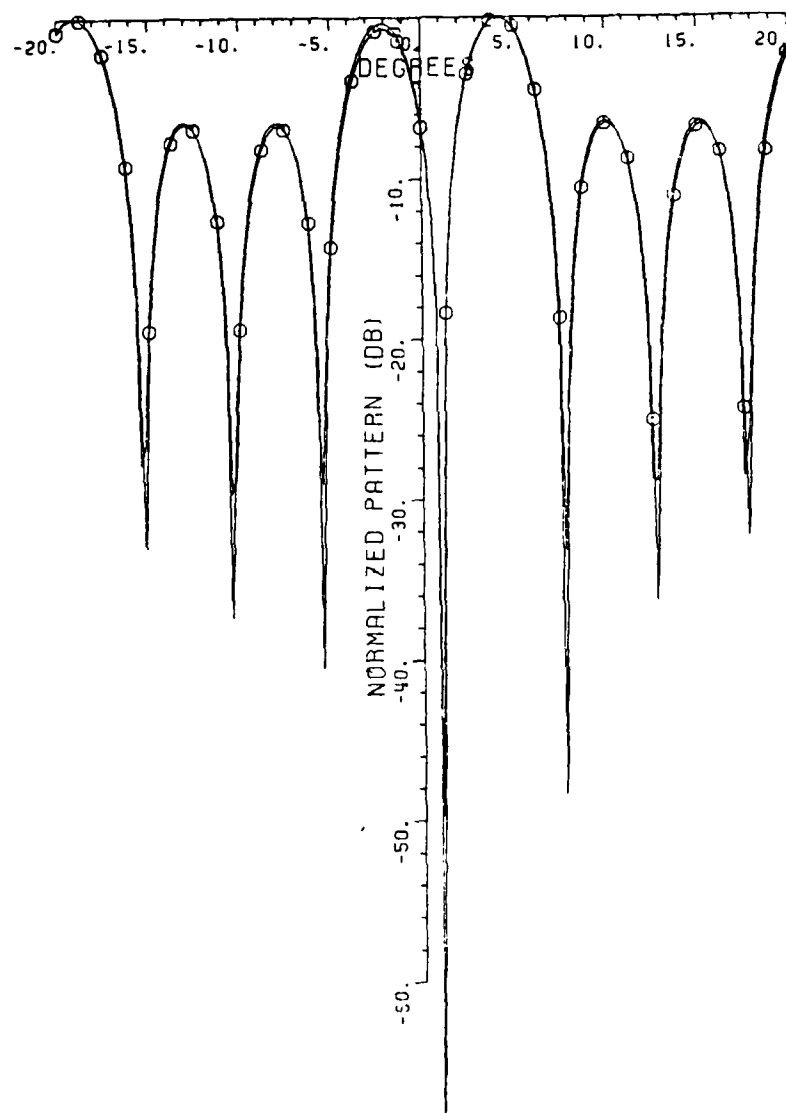


Figure 15. Sum and difference patterns for 5 element array with  
inter-element spacing  $2.5\lambda$ .

Steering angle  $\theta_{exp}=1.2^\circ$

Jammer with power  $P_j=30$  dBN at  $\theta_j=1^\circ$

are similar to those of a monopulse system. The null of the difference pattern coincides with the peak of the sum pattern, and they both point at the expected AoA.

Moving the jammer closer to the expected AoA causes only a slight distortion of the sum and difference patterns until the jammer falls within the mainbeam of the array. In Figures 11-13 the jammer is at  $4^\circ$  while the beam is steered at  $-2^\circ$ ,  $-0.4^\circ$  and  $1.2^\circ$  respectively. Note that the patterns are not distorted much for  $-2^\circ$  and  $-0.4^\circ$ , but for a  $1.2^\circ$  steering angle the difference pattern is highly distorted and the sum pattern does not have its maximum at the intended steering angle.

Figures 14 and 15 display the patterns resulting when a jammer is well within the 3 dB beamwidth, namely at  $1^\circ$  or a quarter of a beamwidth away from the desired signal, and the steering angle is at  $1.2^\circ$  which essentially points at the jammer. The jammer captures the null of the difference pattern for both  $P_j=10$  dBN and  $P_j=30$  dBN. The high powered jammer captures the first null of the sum pattern as well and creates a major distortion of both sum and difference patterns. This null capture may be responsible for the significant estimation error of the monoestimator when the expected AoA is closer to the jammer than to the desired signal and a much better behavior when the sum and difference beams are scanned away from the jammer, e.g., pointing toward negative angles while the desired signal is at zero and the jammer at positive angles. Other conclusions that can be drawn from the figures are that the sum beam optimizes the reception of the signal from the expected AoA and consequently a good initial angle, within a quarter of a beamwidth,

is important. The difference beam is strongly affected by the jammer and thus its null direction is usually biased. Nevertheless the resulting estimates of the monoestimator are quite good for a variety of jammer locations as long as the initial or expected AoA is reasonably accurate.

### c) AoA Estimation in the Presence of Two Jammers

We consider now the estimated AoA in the presence of two jammers. The desired signal is placed at  $\theta=0^\circ$ . One of the jammers is fixed at  $6^\circ$  while the other jammer is located at varying angular distances from the desired signal. The estimated AoA is shown in Figure 16 as a function of the second jammer direction. Comparing the estimates with that of Figures 3 and 5, one finds that the quality of the estimate is about the same as in the presence of one jammer. The additional jammer (fixed at  $6^\circ$ ) does not seem to degrade the performance of the two estimators. The reason for the lack of degradation in performance is that the additional jammer is at a large angular distance (over a beamwidth) from the desired signal AoA. When the two jammers are within a BW of the desired signal AoA their effect is, of course, much more pronounced. Figures 17 and 18 show the plot of the Q-function as a function of the scan angle. In Figure 17 one of the jammers is at a large angular separation from the desired signal ( $8^\circ$  or 2 beamwidths), while in Figure 18 both jammers are within a BW of the desired signal. Note that in Figure 18 the minimum is not as sharp as that in Figure 17 and is displaced from the true AoA. One solution to this problem is to increase the array size. Figure 19 shows the Q-function plot for a 10

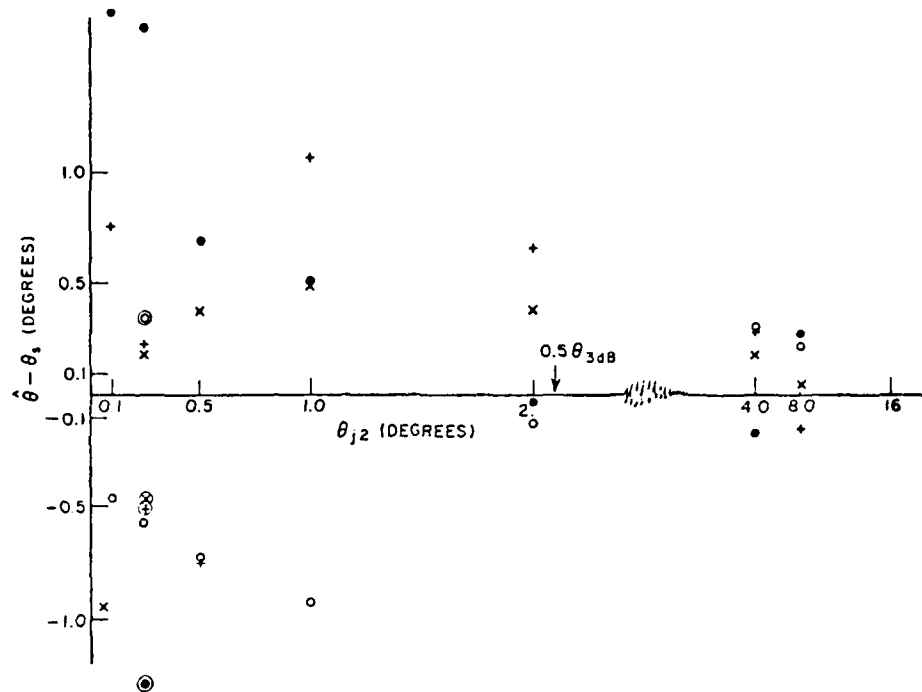


Figure 16. Estimated AoA in the presence of two jammers using a 5 element array as a function of second jammer direction. Averaged over 20 samples.

Signal Power  $P_S=10$  dBN

Jammer Power  $P_{j1}=30$  dBN, jammer fixed at  $\theta_{j1}=6^\circ$

$P_{j2}=10$  dBN.

- $\hat{\theta}_{\text{Mono}}$  resulting from expected AoA of  $-2^\circ$
- x  $\hat{\theta}_{\text{Mono}}$  resulting from expected AoA of  $-0.4^\circ$
- +  $\hat{\theta}_{\text{Mono}}$  resulting from expected AoA of  $+1.2^\circ$
- o  $\hat{\theta}_Q$  for angular sampling density of  $1.6^\circ$

⊙, ⊗, ⊕, and ⊙:  $\hat{\theta}$  for  $P_{j1}=10$  dBN,  $P_{j2}=30$  dBN

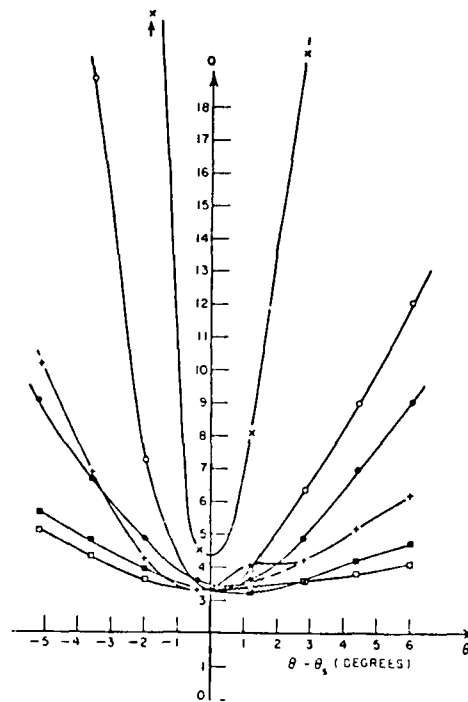


Figure 17. Plots of the Q-function averaged over 10 samples and estimated AoA for different scenarios. 5 element array at  $2.5\lambda$  ( $\theta_{3dB}=4.2^\circ$ ). Angular sampling interval  $1.6^\circ$  for  $\theta_Q$ . Desired signal power  $P_S=10$  dBN, true AoA  $\theta_S=0^\circ$ . Jammer powers:  $P_{j1}=30$  dBN, jammer fixed at  $\theta_{j1}=8^\circ$ .

x  $P_{j2}=30$  dBN,  $\theta_{j2}=6.9^\circ$

o  $P_{j2}=30$  dBN or 50 dBN,  $\theta_{j2}=2^\circ$

+  $P_{j2}=30$  dBN or 50 dBN  $\theta_{j2}=1^\circ$

□  $P_{j2}=30$  dBN or 50 dBN,  $\theta_{j2}=0.5^\circ$

■  $P_{j2}=50$  dBN,  $\theta_{j2}=-0.5^\circ$

●  $P_{j2}=30$  dBN or 50 dBN,  $\theta_{j2}=-1^\circ$



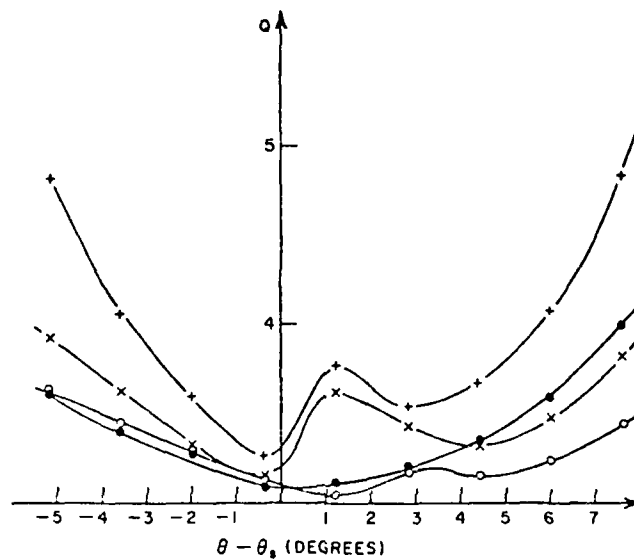


Figure 18. Plots of the Q-function averaged over 10 samples.

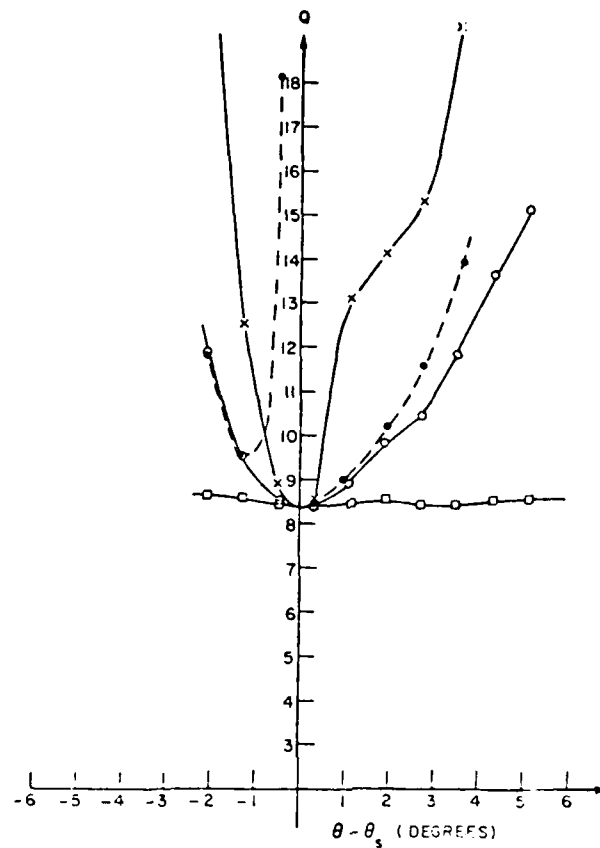
5 element array at  $2.5\lambda$  ( $\theta_{3dB}=4.2^\circ$ ). Angular sampling interval  $1.6^\circ$  for  $\theta_Q$ . Desired signal power  $P_S=10$  dBN, true AoA  $\theta_S=0^\circ$ . Jammers: jammer 1 fixed at  $\theta_{j1}=2^\circ$ .

x  $P_{j1}=30$  dBN;  $P_{j2}=30$  dBN,  $\theta_{j2}=1^\circ$

o  $P_{j1}=30$  or  $50$  dBN;  $P_{j2}=30$  dBN,  $\theta_{j2}=0.5^\circ$

●  $P_{j1}=30$  or  $50$  dBN;  $P_{j2}=30$  dBN,  $\theta_{j2}=-1.0^\circ$

+  $P_S=20$  dBN;  $P_{j1}=50$  dBN;  $P_{j2}=30$  dBN,  $\theta_{j2}=0.5^\circ$



element array ( $BW=2.1^\circ$ ). The samples are taken at double the previous rate since the beamwidth is halved. The estimates are good for two close in jammers, the fixed jammer, however is only slightly inside the 3 dB beamwidth so the performance should be good.

#### 4.2 Estimated Covariance Matrix

In this section the estimation of the AoA is carried out based on an estimated covariance matrix rather than a known one. Most of the results presented are for the Q-estimator, since the monoestimator yields about the same performance for the estimated covariance matrix case as for the known covariance matrix as long as the initial or "guess" angle is fairly good. In general the influence of the matrix estimation is small as long as the number of independent time samples  $N_s$  used is high enough. The minimum number of time samples necessary in order to insure that the covariance matrix is nonsingular equals the number of antenna elements,  $L$ . Good results are achieved for values of  $N_s$  between  $L$  and  $2L$ .

In the figures depicting the Q-function or  $Q_1$ -function the continuous lines correspond to the case for the highest number of samples and also the "known covariance" matrix used for estimation, while the sparsest (dashed) lines correspond to the case when the fewest time samples have been used in the estimation of  $\hat{M}$ . Thus the dash-dot line corresponds to the intermediate number of samples. The number of samples used for obtaining the AoA estimates shown are 5, 10 and 0 respectively. The "0" corresponds to the known covariance matrix.

#### a) AoA Estimation in the Absence of All Jammers

Figure 20 shows the estimated AoA using the monoestimator in the absence of all jammers. The input desired signal-to-noise ratio is 10 dB per element. Results are given for different numbers of time samples used in the estimation of  $\hat{M}$ . Estimated AoA's using a known covariance matrix are also shown. Note that the accuracy of the estimated AoA when the number of samples is equal to the number of elements is just as good as that for the known covariance matrix. This is also true for the Q-estimator (Figures 21 and 22).

When comparing the different figures note that the scale used for the Q-function is in dB--normalized relative to individual noise per element, that is the Q-function of Equation (22) is expressed directly in dB.

In Figure 21, the Q-function is plotted as a function of the scanning direction, while Figure 22 gives the plot of the  $Q_1$ -function. Note that the Q-function has a sharper minimum than the  $Q_1$ -function. But the Q-function involves more calculations (Equation (22)). It involves approximately  $L(L+1)$  extra multiplications per time sample. The array under consideration has five elements and for high input signal-to-noise ratio per element ( $\sim 10$  dB), as anticipated in a TDMA-system, the number of time samples can be chosen rather small. The  $Q_1$ -function will, therefore, not be considered in the calculation of the estimated AoA.

#### b) AoA Estimation in the Presence of One Jammer

Figure 23 shows plots of the Q-function and the Q-estimates of the

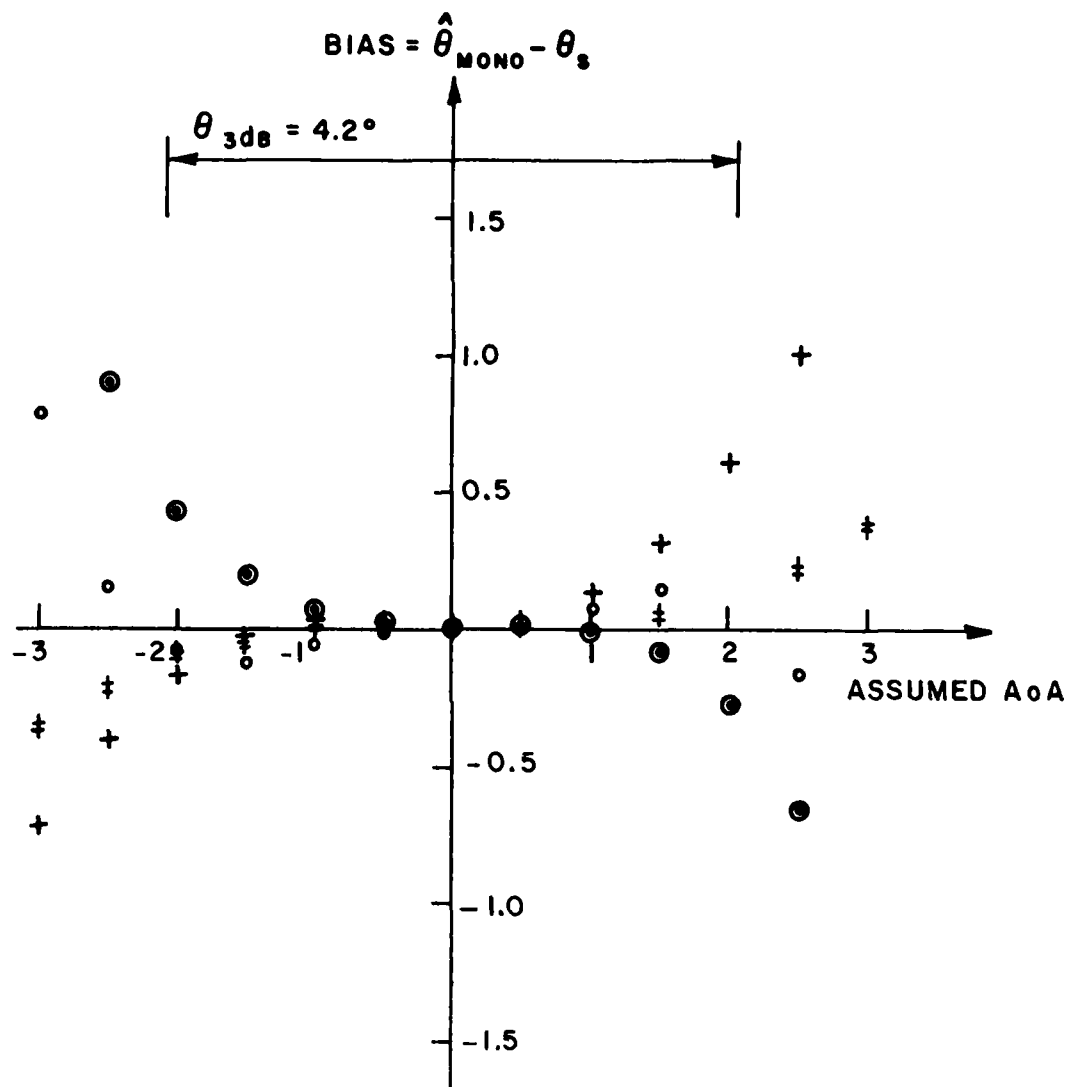


Figure 20. Estimated AoA as a function of the assumed AoA for the monoestimator. Averaged over 20 samples,  $P_s=10$  dBN,  $\theta_s=0^\circ$ . No jamming. 5 element array. +  $\hat{M}(6)$ , x  $\hat{M}(9)$ , o  $\hat{M}(12)$ ,  $\odot$  M known.

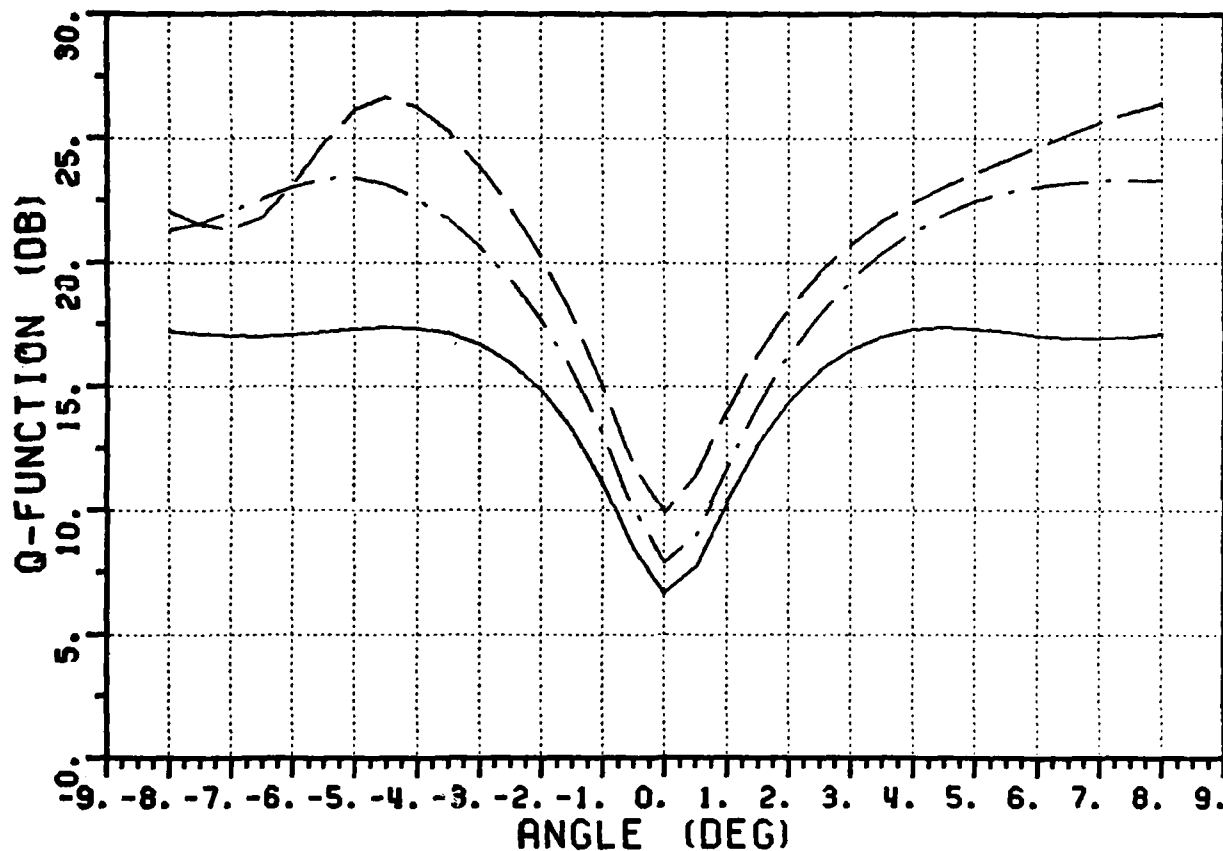


Figure 21. Q-function versus  $\theta$  for 5 element array. Averaged over 5 samples.  $P_s=10$  dBN,  $\theta_s=0^\circ$ , No jamming.

NR of Samples for Matrix:    5    10    0

Estimated AoA: (Deg) :    0.04   0.10   0.08

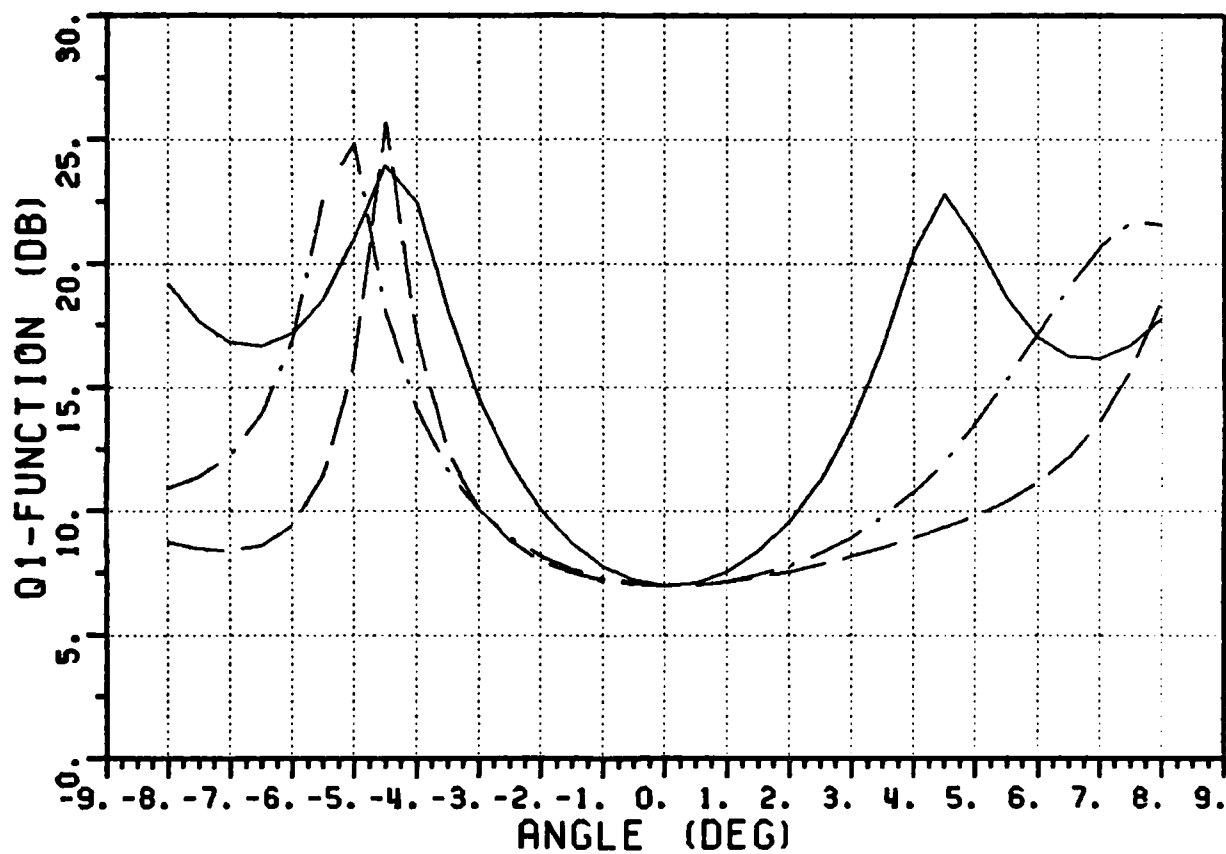


Figure 22.  $Q_1$ -function versus  $\theta$  for 5 element array. Averaged over 5 samples.  $P_S=10$  dBN,  $\theta_S=0^\circ$ , No Jamming.

NR of Samples for Matrix:	5	10	0
Estimated AoA: (Deg):	0.04	0.11	0.08

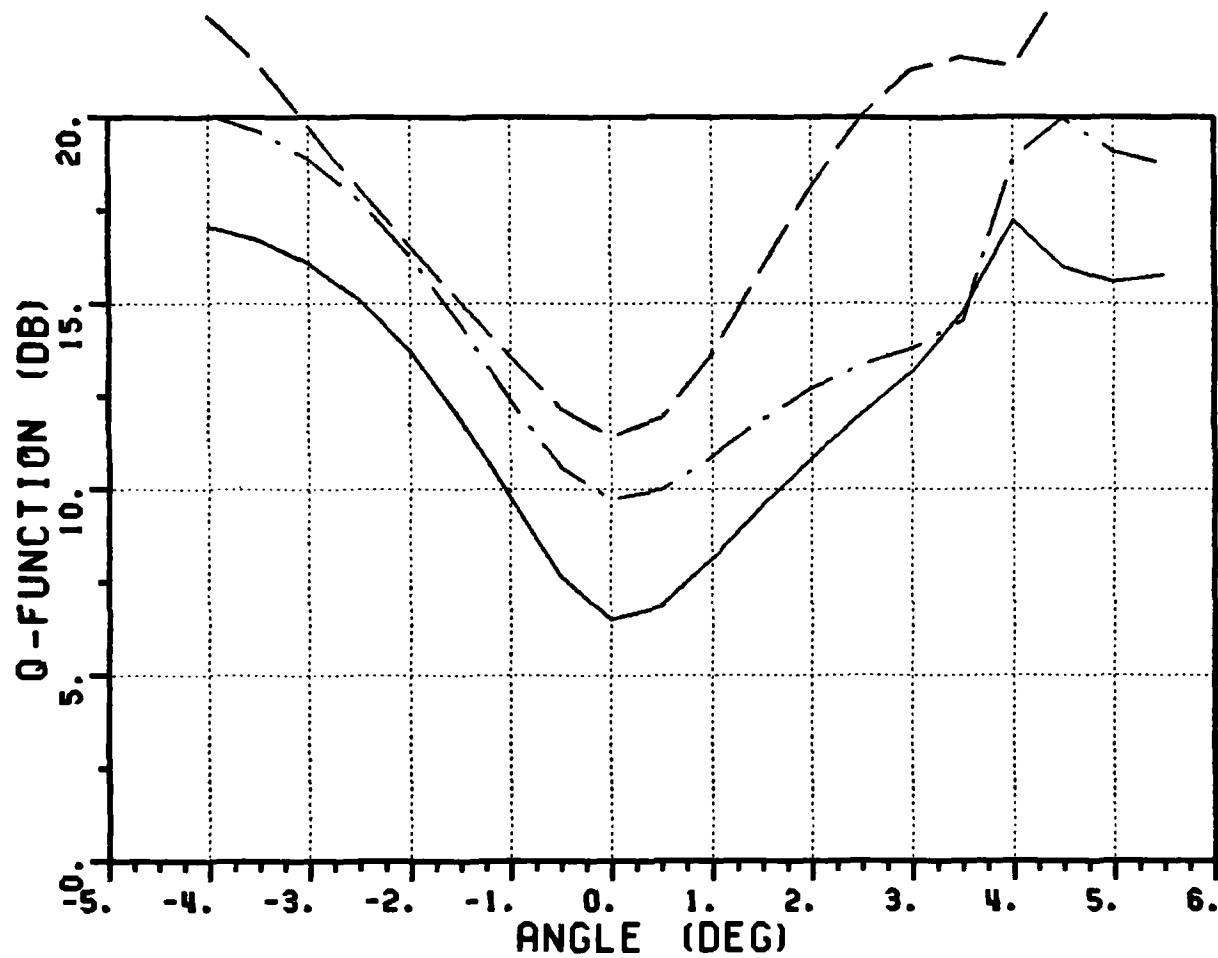


Figure 23. Q-function versus  $\theta$  for 5 element array in the presence of one jammer. Averaged over 5 samples.  $P_S=10$  dBN,  $\theta_S=0^\circ$ ,  $P_J=10$  dBN,  $\theta_J=4^\circ$ .

NR of Samples for Matrix: 5 10 0

Estimated AoA: (Deg): 0.06 0.14 0.14



AoA in the presence of a single jammer when the jammer and the desired signal are at an angular separation of approximately one beamwidth. The jammer-to-noise ratio at each element is 10 dB. Note that the estimate using the estimated covariance matrix is as good as when using the known covariance matrix. The Q-function has a well defined minimum. Figure 24 shows the result when the jammer is moved closer to the desired signal (angular separation  $1^\circ$ ). Note that the minimum is less pronounced, and the estimated AoA is less accurate.

In Figure 25, the jammer-to-noise ratio is increased to 30 dB while the separation between the jammer and the desired signals is still  $1^\circ$ . Note that the difference between the true AoA and the estimated AoA has increased. Thus a close strong jammer reduces the accuracy of the AoA estimate. Again the estimate using the estimated covariance matrix produces a less accurate result than the estimate using a known covariance matrix.

### c) AoA Estimation in the Presence of Two Jammers

Figure 26 shows a plot of the Q-function and the estimated AoA using the Q-estimator in the presence of two strong jammers. Both jammers are at angular separations of more than one beamwidth from the desired signal. Note that the minimum of the Q-function is well defined and the estimated AoA is quite accurate (within 10 percent of the 3 dB beamwidth). Thus, as observed for the known covariance matrix case the array can take care of two jammers outside its mainbeam. Further, the accuracy of the estimated AoA using the estimated and the known covariance matrices is the same.

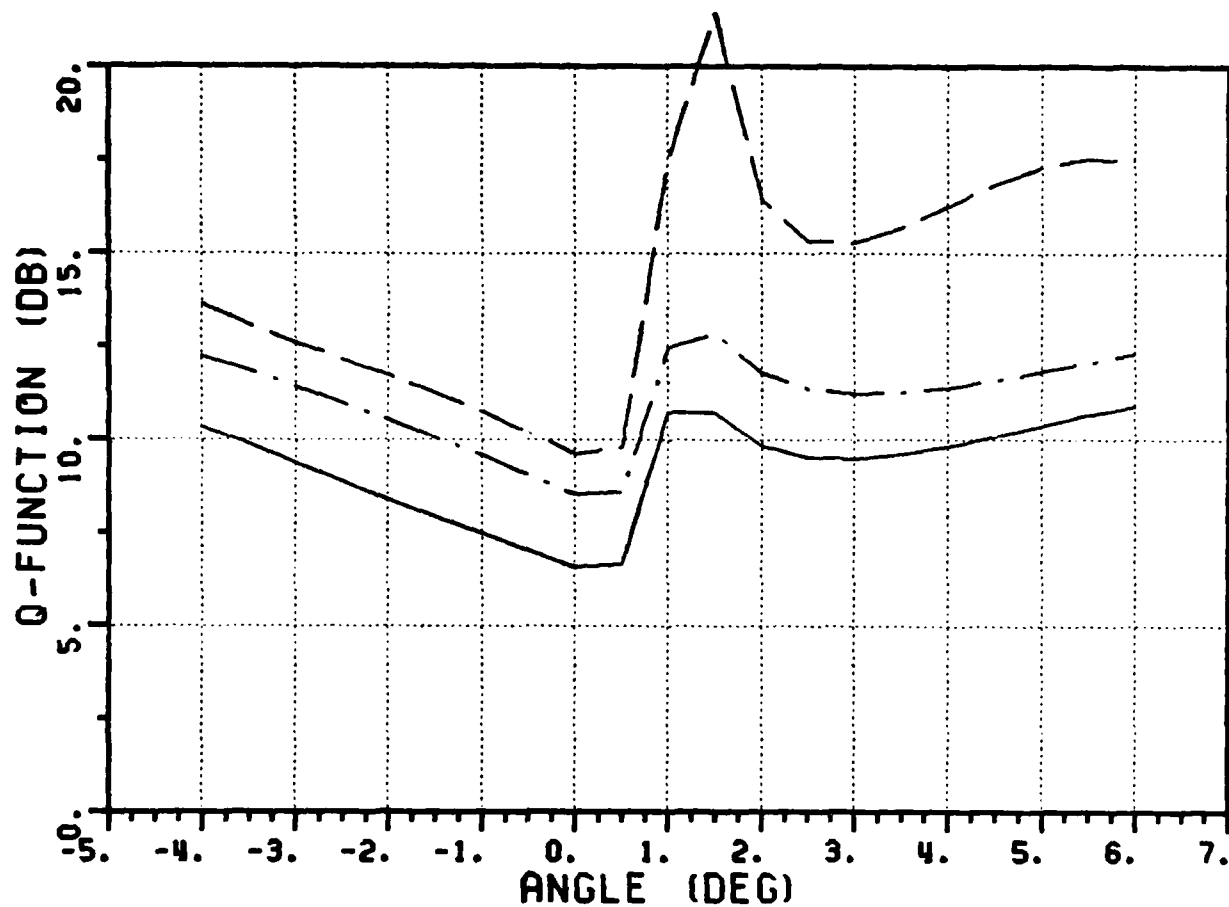


Figure 24. Q-function versus  $\theta$  for 5 element array in the presence of one jammer. Averaged over 5 samples.  $P_s=10$  dBN,  $\theta_s=0^\circ$ ,  $P_j=10$  dBN,  $\theta_j=1^\circ$ .

NR of Samples for Matrix: 5 10 0

Estimated AoA: (Deg): 0.14 0.21 0.18

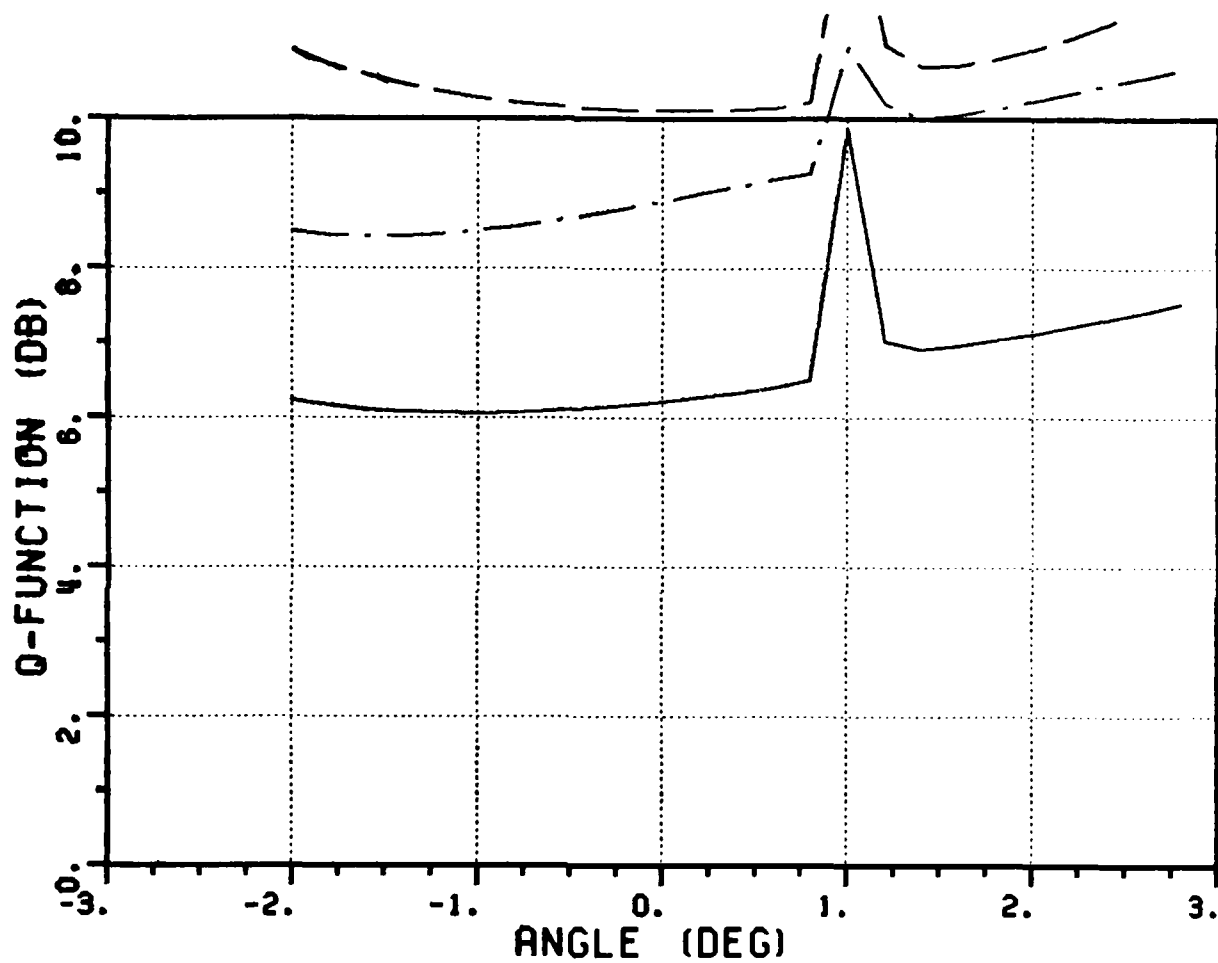


Figure 25. Q-function versus  $\theta$  for 5 element array in the presence of one jammer. Averaged over 5 samples.  $P_S=10$  dBN,  $\theta_S=0^\circ$ ,  $P_J=30$  dBN,  $\theta_J=1^\circ$ .

NR of Samples for Matrix: 5      10      0  
 Estimated AoA: (Deg):    0.07   -1.54   -1.08

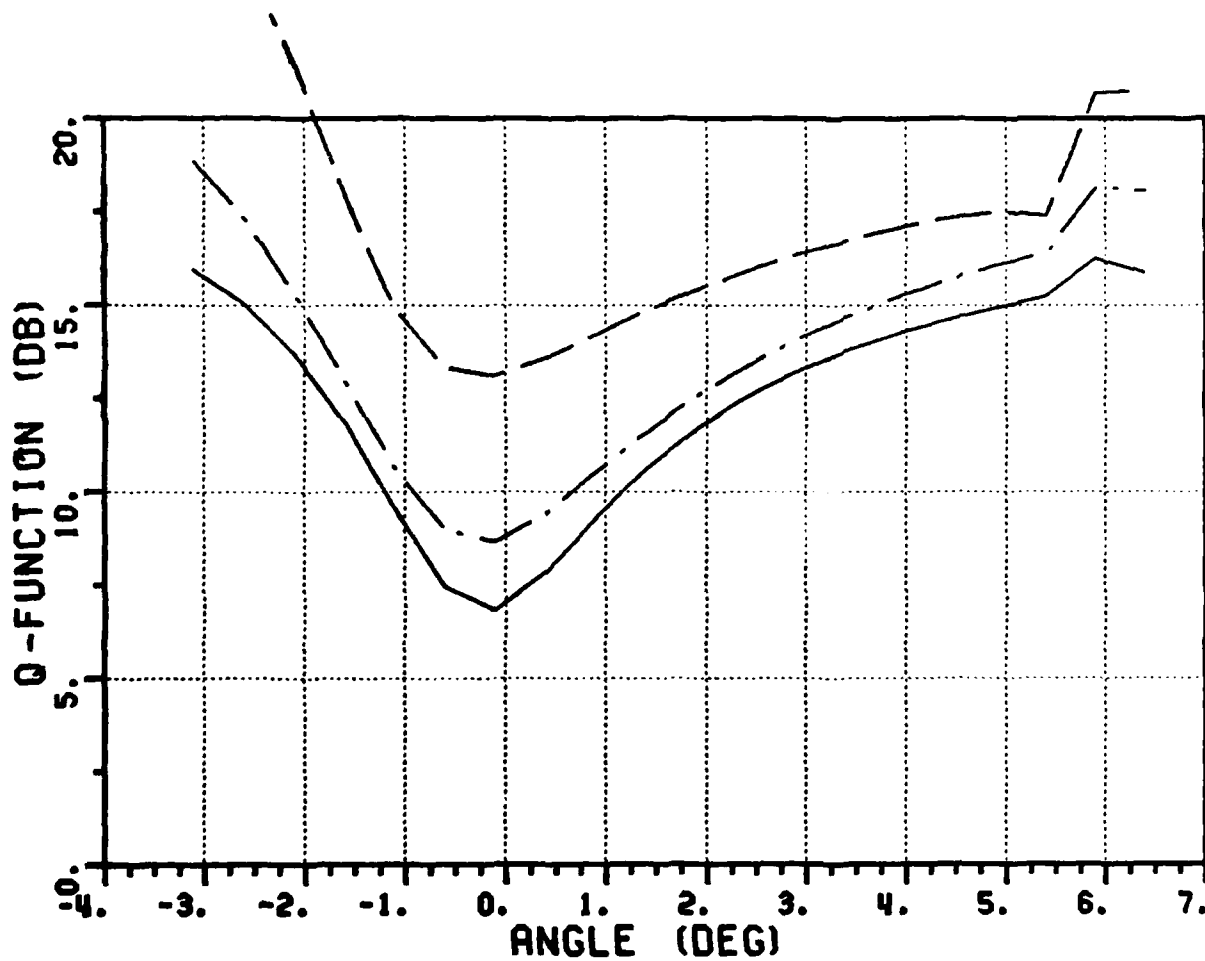


Figure 26. Q-function versus  $\theta$  for 5 element array in the presence of two jammers. Averaged over 5 samples.  $P_S=10$  dBN,  $\theta_S=0^\circ$ ,  $P_{J1}=30$  dBN,  $\theta_{J1}=6^\circ$ ,  $P_{J2}=30$  dBN,  $\theta_{J2}=8^\circ$ .  
 NR of Samples for Matrix: 5 10 0  
 Estimated AoA: (Deg): -0.19 -0.20 -0.16

In Figure 27, one of the jammers is moved inside the main beam of the array. The performance of the array is the same as in the presence of a single incident jammer inside the main beam. The minimum is less pronounced and the estimated AoA is not as accurate as in Figure 26 (where both jammers are outside the main beam). The accuracy of the estimated angle is strongly dependent on the accuracy of the estimated covariance matrix. It can be seen that the angle of arrival error drops by a factor of two as the number of samples used to estimate the covariance matrix is doubled. It again is halved when the exact or known covariance matrix is used. This is in contrast with previous results when the jammers were outside the main beam. Under those conditions the AoA estimate was essentially independent of the number of samples used in estimating the covariance matrix. It appears that with jammers well within the main beam, the effective desired signal to jammer plus noise ratio deteriorates to the point that minor errors in the covariance matrix have a significant affect on the final estimate. The same phenomenon is evident in Figure 28 where both jammers are within the main beam. The accuracy of the estimate deteriorates further and is strongly dependent on the number of samples used in the covariance matrix estimation. Even 10 samples, although yielding better results than 5 samples, do not reduce the error significantly, a larger sample size is apparently needed since for the exact or known covariance the error drops by a factor of three down to a tenth of a beamwidth. It should be noted, however, that even with this difficult scenario the AoA estimate with a 10 sample average is in error only a quarter of a 3 dB beamwidth.

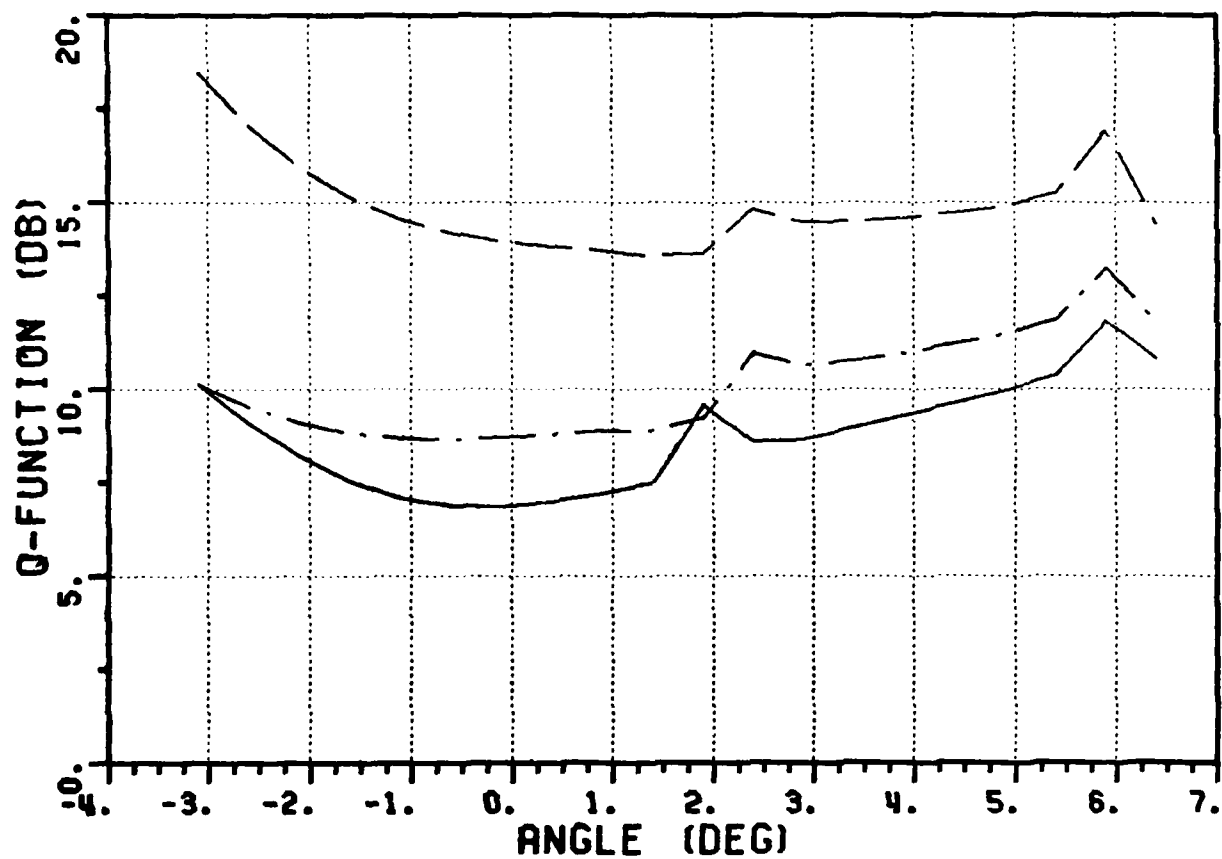


Figure 27. Q-function versus  $\theta$  for 5 element array in the presence of two jammers. Averaged over 5 samples.  $P_S=10$  dBN,  $\theta_S=0^\circ$ ,  $P_{J1}=30$  dBN,  $\theta_{J1}=2^\circ$ ,  $P_{J2}=30$  dBN,  $\theta_{J2}=6^\circ$ .  
 NR of Samples for Matrix: 5 10 0  
 Estimated AoA: (Deg): 1.46 -0.65 -0.30

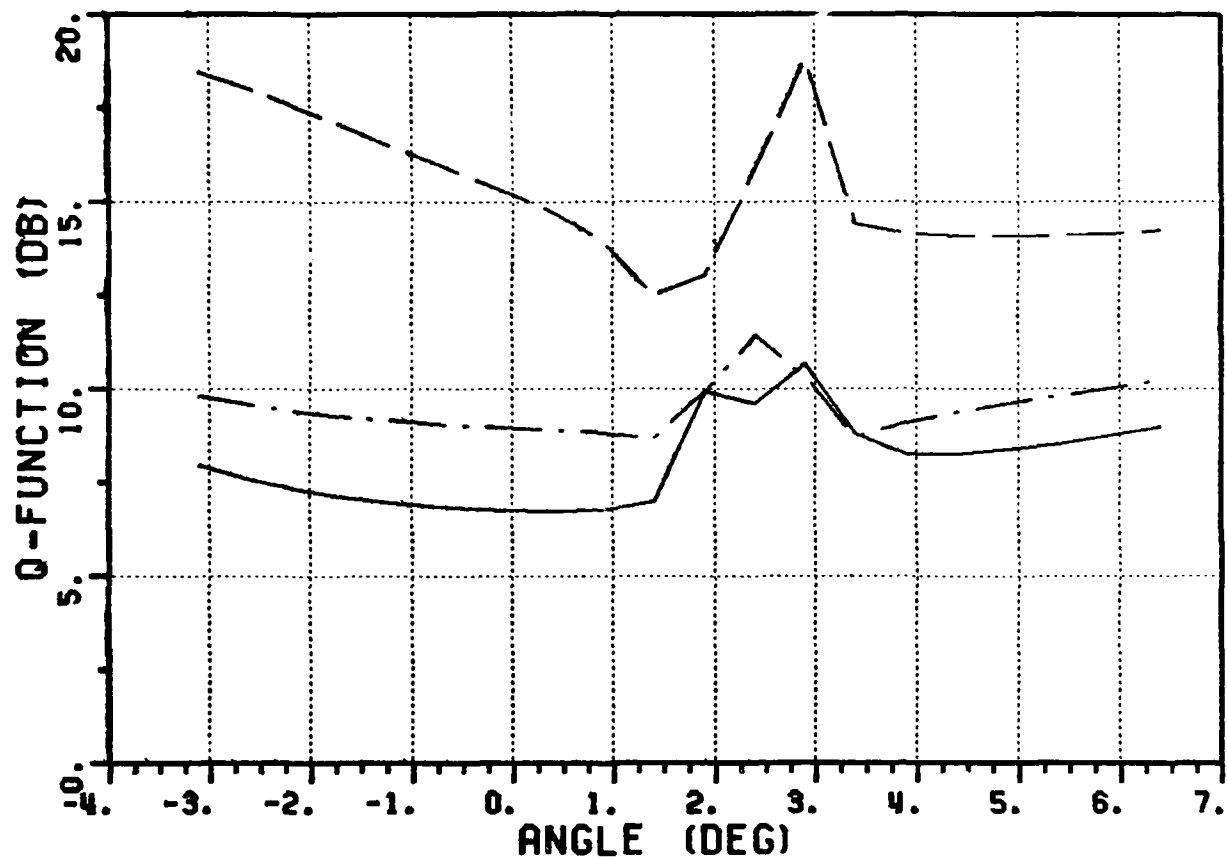


Figure 28. Q-function versus  $\theta$  for 5 element array in the presence of two jammers. Averaged over 5 samples.  $P_S=120$  dBN,  $\theta_S=0^\circ$ ,  $P_{J1}=30$  dBN,  $\theta_{J1}=2^\circ$ ,  $P_{J2}=30$  dBN,  $\theta_{J2}=3^\circ$ .

NR of Samples for Matrix: 5 10 0

Estimated AoA: (Deg): 1.53 1.20 0.43

## 5. SUMMARY AND CONCLUSIONS

The objective of this work was to find a method for the AoA estimation of a desired signal in the presence of multiple jammers. The AoA was to be estimated in the presence of jammers at various angular distances to the desired signal, including close-in jammers.

Two estimators, a monoestimator and a Q-estimator based on the maximum likelihood estimate were studied. Both estimators use the covariance matrix of the element signals. During the estimation of the covariance matrix the desired signal was assumed to be absent. This requirement can be satisfied in a TDMA system since the timing of the uplink (desired) signals are accurately controlled.

The monoestimator is a local estimator and in the absence of all jammers performs like a monopulse system. It requires, however, a prior knowledge of the AoA (within half a beamwidth) of the desired signal. If the expected AoA is not within a half beamwidth of the true AoA, the monoestimator generally breaks down. Such a priori knowledge is not always available, as in the case of mobile terminals (the system beamwidth is kept small to keep the jammers outside the main beam and provide high gain). The monoestimator can, however, be beneficial as a method to improve a preliminary estimate achieved by some other techniques. Some knowledge of the jamming scenario can also be used to improve the accuracy of the monoestimator.

The Q-estimator is a global estimator, in the sense that no previous knowledge of the AoA of the desired signal is needed. It gives very accurate estimates of the AoA, to within a tenth of a beamwidth, as



long as the jammers are not inside the mainbeam of the array. But even for close-in jammers the estimated AoA is still within a quarter of a beamwidth. If further accuracy is required, this estimate can be used to provide the preliminary estimate for the monoestimator.

The effect of an estimated covariance matrix ( $\hat{M}$ ) on the estimated AoA was also studied. It was found that the number of independent sample element signals used to estimate the covariance matrix should be somewhat larger than the number of array elements ( $L$ ). The Q-estimator using the estimated covariance matrix gave very accurate estimates for jammers outside the mainbeam of the array. As the angular separation between the jammers and the desired signal decreased the estimates deteriorated somewhat, but still were within a quarter of a beamwidth of the array. The monoestimator did not degrade significantly as long as the "expected" angle was within a quarter of a beamwidth of the true angle.

#### REFERENCES

- [1] Davis, R.C., L.E. Brennan and L.S. Reed, "Angle Estimation with Adaptive Arrays in External Noise Fields," IEEE Trans. Aerosp. Elect. Syst., Vol. AES-12, March 1976.
- [2] McGarty, T.P., "The Effect of Interference Signals on the Performance of Angle of Arrival Estimates," IEEE Trans. Aerosp. Electronics Syst., Vol. AES-10, January 1974.
- [3] El-Behery, I.N. and R.H. MacPhie, "Maximum Likelihood Estimation of Source Parameters from Time-Sampled Outputs of a Linear Array," J. Acoust. Soc. Am., Vol. 62, No. 1, July 1977.
- [4] Ksienski, A.A. and R.B. McGhee, "A Decision Theoretic Approach to the Angular Resolution and Parameter Estimation Problem for Multiple Targets," IEEE Trans. Antennas and Propagation, Vol. AES-4, May 1968, pp. 443-455.
- [5] Applebaum, S.P., "Adaptive Arrays," IEEE Trans. Antennas and Propagation, Vol. AP-24, No. 5, September 1976, pp. 585-598.



## *MISSION of Rome Air Development Center*

*RADC plans and executes research, development, test and selected acquisition programs in support of Command, Control Communications and Intelligence (C<sup>3</sup>I) activities. Technical and engineering support within areas of technical competence is provided to ESD Program Offices (POs) and other ESD elements. The principal technical mission areas are communications, electromagnetic guidance and control, surveillance of ground and aerospace objects, intelligence data collection and handling, information system technology, ionospheric propagation, solid state sciences, microwave physics and electronic reliability, maintainability and compatibility.*

4-8  
DT